

Acoustic Filters to Aid Digital Voice*

By J. L. FLANAGAN

(Manuscript received September 19, 1978)

Digital conversion of speech requires that the signal be band-limited. The band limitation customarily is accomplished by electrical filtering. Typically, the cost of electrical filtering is a noticeable fraction of the total cost of voice digitization. We propose here that a large part, if not all, of the requisite filtering can be economically accomplished through acoustic design of the transducer housing (both at transmitter and receiver). We derive a design technique for voice-band acoustic filters, and we compute and construct several prototype filters. We make free-space acoustic measurements on the prototypes, used in combination with electret microphones. Finally, we demonstrate that the acoustic filters can approximate the band-limit specifications for the D-channel bank.

I. DIGITAL CONVERSION OF ACOUSTIC SIGNALS

The well-known sampling theorem prescribes that a signal can be exactly recovered from its time-discrete samples provided the samples are taken at least as frequently as twice the rate of the highest frequency component present in the signal. Band limitation of signals is therefore fundamental to distortion-free digital representation. The same band limitation is necessary to recover the continuous signal from its time-discrete samples. High quality analog-to-digital (A/D) and digital-to-analog (D/A) conversions consequently depend upon band limitation sufficient to suppress spectral aliasing.

Electrical filters typically are used to provide the requisite band limitation. Traditionally, these have been analog implementations, but new advances in integrated circuitry permit implementation through high-rate sampling, digital filtering, and decimation. Still, at the initial and final analog levels, the signal must be analog band-limited, and

* An abridged report of this work was presented to the 96th meeting of the Acoustical Society of America, J. Acoust. Soc. Am., 64 (November 1978), p. S55.

the total band limitation must be accomplished sufficiently well to suppress aliasing.

To illustrate a typical need for band-limiting, recall that in T-carrier digitization of voice signals the signal bandwidth is limited to less than 4 kHz and the sampling rate is 8 kHz. In terms of this requirement, most of our telephone transmitters (microphones) are too good. Figure 1 shows approximate frequency responses for the Western Electric T-1 carbon button and the EL-2 electret.^{1,2} These microphones have high-frequency responses that extend much above 4 kHz, and the rate of attenuation above this point is typically shallow, about 12 dB/oct. Overt low-pass filtering, to approximately the sixth order, is necessary to restrict the transduced signal to a bandwidth suitable for sampling at 8 kHz. This band-limiting is typically done by electrical filtering.

As the cost of integrated digital converters (A/D and D/A) continues to diminish, the cost of electrical filtering, especially analog, becomes a significant part of the expense of digital conversion.¹ This issue is particularly important in systems where digitization must be performed on a dedicated per-channel basis. Typical instances include digital mobile radio telephone and digital subscriber loop systems, where voice digitization is accomplished at, or close to, the station set. In these cases, there is considerable incentive to reduce the cost of signal filtering and digitization. In other cases, where group digitization and multiplexing at a central location are done, the per-channel costs are less dominant. Also, if digitization is performed at a central location following an analog transmission of significant distance, additional filtering may be needed to control accumulated electrical noise.

II. ACOUSTIC BAND-LIMITING FILTERS

One possibility for gaining cost advantages is to make the acoustic transducer do some, or preferably all, the signal filtering—both for sampling (at the transmitter) and desampling (at the receiver). To

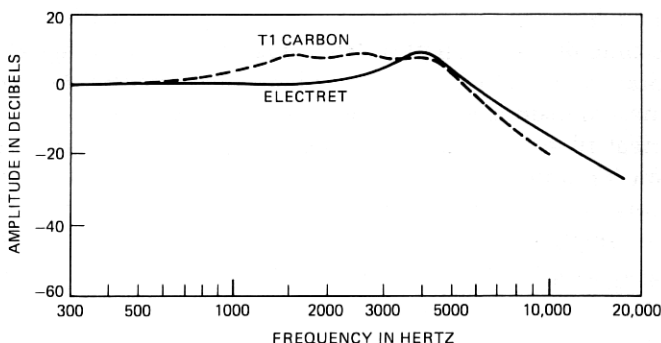


Fig. 1—Approximate frequency responses for the T1 carbon and EL-2 electret microphones.

incorporate this filtering as part of the internal mechanics of a microphone or earphone is not so attractive because it reduces the versatility of these transducers for a variety of applications in voice communications. But to install the broadband transducer in an acoustic housing that could implement the band filtering and that might easily be injection-molded (say, as part of the transmitter cap in the handset) or stamped out (as part of the transducer case) is attractive, both functionally and economically.

This report, therefore, sets forth a design technique for producing simple acoustic filters for voice transmission. The acoustic filters can be applied onto typical telephone transducers and can provide low-pass band-limiting which closely approximates the D-channel bank requirements for voice digitization.

In this report we discuss transmitter (microphone) filters only, but similar principles apply for desampling filters at the receiver (earphone or loudspeaker).

III. SOME ACOUSTIC THEORY RELEVANT TO FILTER DESIGN

It is convenient to focus our discussion on acoustic analyses that can be formulated primarily in terms of one-dimensional sound propagation. That is, to keep the discussion simple, we will not make detailed treatment of cross-modes.* With this in mind, recall that the spatial and temporal variations of sound pressure, $p(x, t)$, and volume velocity, $U(x, t)$, for lossless, one-dimensional sound propagation in a rigid, uniform conduit of cross-sectional area A are described by

$$\begin{aligned}\frac{\partial p}{\partial x} &= -\frac{\rho}{A} \frac{\partial U}{\partial t}, \\ \frac{\partial p}{\partial t} &= -\frac{\rho c^2}{A} \frac{\partial U}{\partial x},\end{aligned}\tag{1}$$

where ρ is the density of the medium (air in our case), and c is the sound velocity.† Eliminating either dependent variable produces the customary wave equation

$$\frac{\partial^2 \xi}{\partial x^2} = \frac{1}{c^2} = \frac{1}{c^2} \frac{\partial^2 \xi}{\partial t^2},\tag{2}$$

* We shall see shortly that we cannot always escape this complexity.

† Typically,

$$\rho = 1.21 \times 10^{-3} \text{ gm/cm}^3$$

$$c = 3.40 \times 10^4 \text{ cm/s.}$$

Further, the shape of the cross section A is unimportant for the lossless case.

which is satisfied both for $\xi = p$ and $\xi = U$.

Sinusoidal time dependence is represented by $\xi(x, t) = \xi(x)e^{j\omega t}$, where ω is the radian frequency. The spatial dependence is then described by the total derivatives

$$\begin{aligned}\frac{dp}{dx} &= -\left(j\omega \frac{\rho}{A}\right)U = -z U, \\ \frac{dU}{dx} &= -\left(j\omega \frac{A}{\rho c^2}\right)p = -y p,\end{aligned}$$

and

$$\frac{d^2\xi}{dx^2} = -\left(\frac{\omega^2}{c^2}\right)\xi = zy \xi. \quad (3)$$

It is not accidental that these look like equations for an electrical transmission line, where p is analogous to voltage and U analogous to current. Though we have written down the conditions for no loss, z and y generally are complex quantities, and represent, respectively, the per-unit-length acoustic impedance and admittance of the rigid conduit, exactly analogous to the electrical line. The one-dimensional wave motion must be composed of progressive waves in $+x$ and $-x$ direction and must satisfy

$$\xi(x) = (\xi_+ e^{-\gamma x} + \xi_- e^{\gamma x}), \quad (4)$$

where $\gamma = \sqrt{zy} = (\alpha + j\beta)$ is the complex propagation constant, and ξ_+ and ξ_- are integration constants determined by boundary conditions. This leads immediately to the result we wish to make use of here.

For a length of conduit, l , eq. (4) permits relating the pressures and volume velocities at each end, namely,

$$\begin{aligned}p_2 &= p_1 \cosh \gamma l - (U_1 Z_0) \sinh \gamma l \\ U_2 &= U_1 \cosh \gamma l - (p_1 / Z_0) \sinh \gamma l,\end{aligned} \quad (5)$$

where the characteristic impedance $Z_0 = \sqrt{z/y}$. This is equivalent to the 4-pole network representation in Fig. 2b, where the series and shunt elements are, respectively,

$$\begin{aligned}z_a &= Z_0 \tanh \gamma l / 2 \\ z_b &= Z_0 \operatorname{csch} \gamma l.\end{aligned} \quad (6)$$

This form will be convenient for the calculations we wish to make. Note one thing further about small values of the length dimension. The series expansions

$$\tanh x = x - \frac{x^3}{3} + \frac{2x^5}{15} \cdots$$

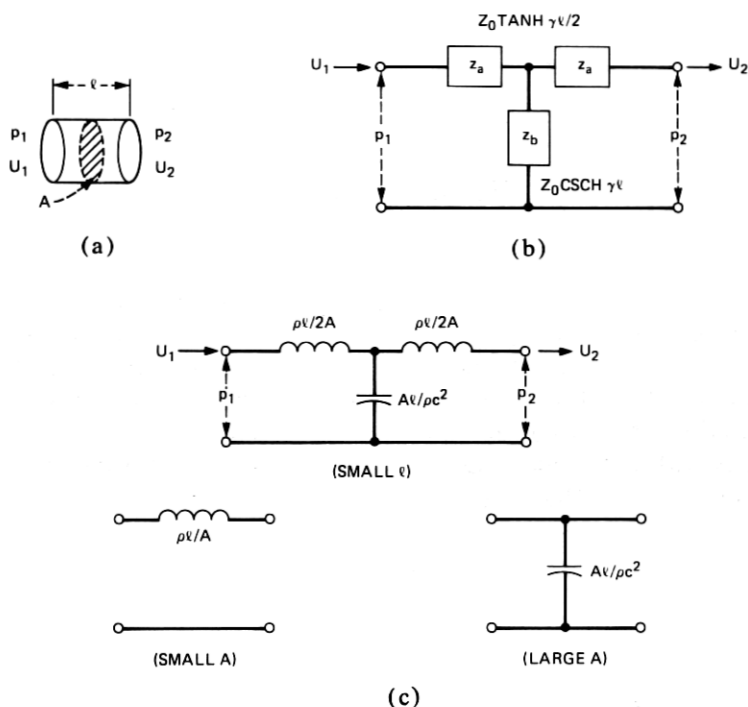


Fig. 2—Lumped constant representation of plane-wave propagation in a length l of right-circular conduit.

$$\sinh x = x + \frac{x^3}{3!} + \frac{x^5}{5!} \dots \quad (7)$$

show that, for $\gamma l \ll 1$, the transcendental quantities can be approximated by lumped elements

$$\begin{aligned} z_a &\cong (z l / 2) \\ z_b &\cong 1 / (\gamma l). \end{aligned} \quad (8)$$

Except for radiation impedances, which typically are small, and for some small-dimension viscous effects, this is all we need to commence a filter design. We specify, without further explanation, appropriate values for the complex per-unit-length acoustic impedance and admittance, namely,

$$\begin{aligned} z &= (R + j\omega L) \\ y &= (G + j\omega C), \end{aligned}$$

where

$$\begin{aligned}
 R &= (S/A^2) \left(\frac{\omega \rho \mu}{2} \right)^{1/2} \\
 L &= \rho/A \\
 G &= S \left(\frac{\eta - 1}{\rho c^2} \right) \left(\frac{\lambda \omega}{2 c_p \rho} \right)^{1/2} \\
 C &= A/\rho c^2,
 \end{aligned} \tag{9}$$

and where S is the inner circumference of the conduit, μ the viscosity coefficient, λ the coefficient of heat conduction, η the adiabatic constant, and c_p the specific heat at constant pressure (all for the filling medium).^{3, 4} As the relations (9) suggest, the loss R is associated primarily with viscous loss and the conductance G is associated primarily with heat conduction loss, both at the conduit walls. Also, for the lossless case, the lumped approximation (8) gives

$$\begin{aligned}
 z_a &= \frac{\rho l}{2A} \\
 z_b &= \frac{Al}{\rho c^2},
 \end{aligned} \tag{10}$$

as shown in Fig. 2c.

It is clear from the relations (6) and (8) that a simple, effective low-pass filter might be fabricated from a sequence of constrictions and reservoirs, as represented in Fig. 3a. Here the cross-sectional area is alternately small and large. To a first approximation, for dimensions small compared with a wavelength, the relations (10) show this structure to be roughly equivalent to the inductance-capacitance (LC) ladder network depicted in Fig. 3b. The design of automobile exhaust mufflers is a simple application of this fundamental notion.

The structure of Fig. 3a can be made more compact by shrinking the length of the small-area inertive (inductive) sections. In the limit $l_L \rightarrow 0$, and the inductor becomes a thin perforated baffle, as shown in Fig. 3c. In this case the inertance of the air in the aperture is conditioned primarily by the radiation reactance of the air load on A_L . Also, the resistive component of this radiation impedance, and viscous effects at small dimensions, dominate the loss characteristics. To examine this behavior, we need to look at the radiation impedance for a circular piston in a baffle.

A piston of radius, a , in a plane baffle, radiating into free space, has a radiation impedance approximated by

$$z_p = \frac{\rho c}{\pi a^2} \left[\frac{(ka)^2}{2} + j \frac{8(ka)}{3\pi} \right], \quad ka \ll 1, \tag{11}$$

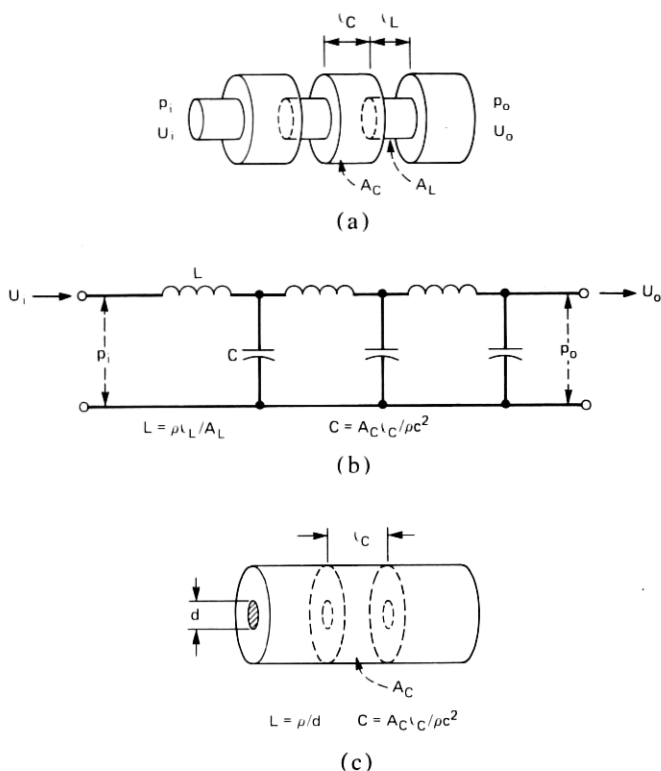


Fig. 3—Acoustic filter composed of alternate constrictions and reservoirs.

where $k = \omega/c$. One sees that the air load on one side of the piston is equivalent to an inductance of

$$\frac{L_a}{2} = \frac{8\rho}{3\pi^2 a} = 0.27 \rho/a. \quad (12)$$

And for two sides radiating (as the perforation in a thin baffle would do into the adjacent cavities), the reactive load is equivalent to an inductance of

$$L_a = 0.54 \rho/a.* \quad (13)$$

This approximation to the inductance of a thin circular constriction is traditionally represented in the literature as

$$L_a \cong \rho/2a = \rho/d.† \quad (14)$$

* Note this implies an equivalent length of the thin constriction $\rho l_e/A = 0.54 \rho/a$, or $l_e = 1.7a$.

† For a vanishingly thin plane baffle of infinite extent.

The viscous loss associated with the aperture can be crudely approximated by the per-unit-length resistance R , given in (9), multiplied by the thickness h of the baffle. A somewhat better empirical approximation to this loss is given by Morse and Ingard³ as

$$R_a = \frac{1}{4\pi a^2} \sqrt{2\rho\omega\mu} \ln\left(\frac{2a}{h}\right). \quad (15)$$

One sees that this loss is relatively small for most dimensions of interest (for example, for $a = 7$ mm and $h = 1$ mm, $R_a < 0.1$ cgs acoustic ohms). Because of this, the damping usually desired in a filter design must be obtained from added loss, such as silk screen or cloth (which typically has a resistance on the order of 3 to 6 cgs ohms for an area of 1 cm²).

Let us summarize, then, the several relations that subsequently will be useful for designing some acoustic filters.

Lumped inductance of a circular aperture of radius a :

$$L_a = \rho/2a$$

Distributed T-section impedances for a length l of uniform conduit of cross-sectional area A :

$$z_a = Z_0 \tanh \gamma l/2$$

$$z_b = Z_0 \operatorname{csch} \gamma l$$

Lumped inductance and compliance for a length l of uniform conduit of cross-sectional area A :

$$L_a = \rho l/A \quad (\text{small } A)$$

$$C_a = Al/\rho c^2 \quad (\text{large } A). \quad (16)$$

These few simple facts, together with estimates of acoustic loss, permit us to proceed with some filter designs. We should, however, keep clearly in mind the distributed nature of the physical system and the expected behavior at small wavelengths. A brief characterization of distributed aspects is worthwhile here and will be useful later.

3.1 Small wavelength effects—cross modes

Specific applications sometimes place constraints on transducer size and may dictate dimensions that can be comparable to a wavelength at the higher frequencies of interest. [Note that the audible frequency spectrum spans about 10 octaves, with wavelengths (in air) of about 1700 cm down to about 2 cm.] One-dimensional wave propagation and lumped-constant approximations to acoustic parameters must, therefore, be used prudently, and with a realization that they do not adequately describe behavior at frequencies where wavelengths are comparable to device dimensions.

For small-amplitude linear wave behavior, the wave equation (2) should properly be written

$$\nabla^2 \xi = \frac{1}{c^2} \frac{\partial^2 \xi}{\partial t^2}, \quad (17)$$

where the ∇^2 operator is taken appropriate to the geometry. Our purpose here is not to give a tutorial on solutions of wave equations, but we need to recall two results that we will need in the subsequent discussion.

3.2 Rectangular geometry

For a rigid-wall enclosure of rectangular geometry, the (unforced) sound pressure $p(x, y, z, t)$ inside the enclosure must satisfy

$$\frac{\partial^2 p}{\partial x^2} + \frac{\partial^2 p}{\partial y^2} + \frac{\partial^2 p}{\partial z^2} = \frac{1}{c^2} \frac{\partial^2 p}{\partial t^2}. \quad (18)$$

For rectangular dimensions l_x, l_y, l_z , and with origin taken at a corner, the solution (to within a multiplicative constant) is

$$p(x, y, z, t) = \cos\left(\omega_x \frac{x}{c}\right) \cos\left(\omega_y \frac{y}{c}\right) \cos\left(\omega_z \frac{z}{c}\right) e^{j\omega t},$$

where

$$\omega = \sqrt{\omega_x^2 + \omega_y^2 + \omega_z^2} \quad (19)$$

and

$$\omega_i = \frac{c}{l_i} n_i \pi, \quad n_i = 0, 1, 2, \dots$$

$$i = x, y, z.$$

These conditions reflect the boundary constraint that a standing wave of pressure must have an antinode at the walls of the enclosure (correspondingly, the particle velocity normal to the walls must be zero). The eigenfrequencies (normal modes of vibration) are, therefore,

$$f = \frac{\omega}{2\pi} = \frac{c}{2} \left[\left(\frac{n_x}{l_x} \right)^2 + \left(\frac{n_y}{l_y} \right)^2 + \left(\frac{n_z}{l_z} \right)^2 \right]^{1/2}. \quad (20)$$

Traditionally, the modes of the enclosure are designated by the indices (n_x, n_y, n_z) .

3.3 Cylindrical geometry

In the same vein, the unforced sound pressure within a cylindrical enclosure must satisfy

$$\frac{1}{r} \frac{\partial}{\partial r} \left(r \frac{\partial p}{\partial r} \right) + \frac{1}{r^2} \frac{\partial^2 p}{\partial \phi^2} + \frac{\partial^2 p}{\partial z^2} = \frac{1}{c^2} \frac{\partial^2 p}{\partial t^2}. \quad (21)$$

For cylindrical dimensions of radius a and length l , the pressure solution (to within a multiplicative constant) is

$$p(r, \phi, z, t) = \cos(m\phi) \cos\left(\frac{\omega_z z}{c}\right) J_m\left(\frac{\omega_r r}{c}\right) e^{j\omega t},$$

where the characteristic values are

$$\omega_z = \left(\frac{\pi n_z c}{l}\right), \quad n_z = 0, 1, 2, \dots$$

and

$$\omega_r = \left(\frac{\pi \alpha_{mn} c}{a}\right), \quad (22)$$

where α_{mn} is the n th root of $(d/d\alpha)[J_m(\pi\alpha)] = 0$. The characteristic radian frequency is

$$\omega = \left(\omega_z^2 + \omega_r^2\right)^{1/2},$$

and the eigenfrequencies are

$$f = \frac{c}{2} \left[\left(\frac{n_z}{l}\right)^2 + \left(\frac{\alpha_{mn}}{a}\right)^2 \right]^{1/2}. \quad (23)$$

Again, the normal modes of the enclosure are traditionally designated by the indices (n_z, m, n) . The normal frequency descriptions of (20) and (23) will be useful to us shortly.

IV. DESIGNS FOR ACOUSTIC LOW-PASS FILTERS

If one examines the responses of typical telephone transducers (as in Fig. 1) against the requirements for voice digitization at 8-kHz sampling, the amount of low-pass band-limiting required suggests a filter of about sixth order. (The electrical filters customarily used are of this order). Our present interest, then, is to achieve this amount of band-limiting with the simplest possible acoustic structure—one that requires minimal fabrication effort and expense and has no particularly critical mechanical tolerances. One such structure is the ladder network that we alluded to earlier. Let us first do the network design, then convert this design into corresponding acoustic parameters, and finally convert these data into a real acoustic filter that can be applied to an existing telephone transducer.

4.1 Sixth-order uniform ladder network

To keep the analysis simple, let us assume that the acoustic radiation load at the input (incident surface) of the filter is small by comparison to the impedance level, and that the acoustic load on the output (typically, the microphone diaphragm) is relatively high. We, therefore, are interested in the high impedance (open-circuit) response of the

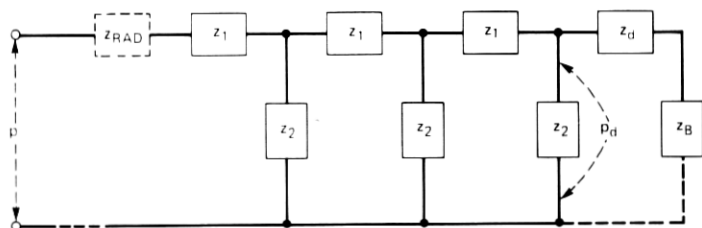


Fig. 4—Lumped network representation for a microphone filter.

filter network to a given input sound pressure, as shown in Fig. 4. The incident sound pressure is p_i and the sound pressure at the microphone diaphragm is p_d . The impedance of the microphone diaphragm and back cavity ($z_d + z_B$) is large compared to the impedance level of the filter elements.

Writing the loop equations for this uniform ladder shows that the frequency response of the transmission function (ratio of Fourier transforms of p_i and p_d) is

$$(p_d/p_i) = \frac{z_2^3}{D},$$

where the system determinant is

$$D = \begin{vmatrix} (z_1 + z_2) & -z_2 & 0 \\ -z_2 & (z_1 + 2z_2) & -z_2 \\ 0 & -z_2 & (z_1 + 2z_2) \end{vmatrix}. \quad (24)$$

Algebraic manipulation gives

$$p_d/p_i = \frac{1}{(x^3 + 5x^2 + 6x + 1)},$$

where

$$x = (z_1/z_2).^* \quad (25)$$

We estimate the three real roots of the denominator of (25) as

$$\begin{aligned} r_1 &= -0.20 \\ r_2 &= -1.57 \\ r_3 &= -3.25. \end{aligned} \quad (26)$$

And we see that this form of network exhibits only poles in its transfer function. If the serial element z_1 were essentially a lossy (resistive) lumped inductance (as would be the case for a relatively small constrict-

* Note this characteristic equation is sixth-degree in frequency, ω .

ing tube or an aperture) and the shunt element z_2 essentially a lossy (conductive) lumped compliance, then

$$(z_1/z_2) \cong (R + sL)(G + sC), \quad (27)$$

and the complex frequencies, s , for which singularities exist in the transfer function are

$$s_i = (-\alpha \pm j\beta_i),$$

where

$$\alpha = \frac{1}{2} \left(\frac{R}{L} + \frac{G}{C} \right)$$

and

$$\beta_i^2 = (\beta_{0i}^2 - \alpha^2) = \left(\frac{RG - r_i}{LC} - \alpha^2 \right), \quad i = 1, 2, 3. \quad (28)$$

That is, the poles occur in three sets of complex conjugates, all with the same damping.*

4.1.1 Calculation of acoustic parameters—uniform ladder

Given these results, together with a prescribed transducer, how do we formulate the acoustical structure?

First we wish to choose the singularities of the filter transfer function so that, when taken in combination with the specified transducer, the combined response meets a particular criterion. We will be guided here roughly by the typical T1-carbon button and the EL-2 electret responses, shown in Fig. 1, and the D-channel bank band-limit specifications. This typically will result in a low-pass filter that attenuates early in frequency to compensate for the characteristic rise in the T1 and EL-2 responses at around 3 to 4 kHz. It is convenient to choose the singularities on the basis of the lumped constant relations (28), but we will remain alert to the distributed nature of the problem so as not to be misled by this simplification.

In accordance with these criteria then, we select values as follows. For relatively low loss ($RG \ll r_i$),

$$\beta_{0i} \cong \left(\frac{r_i}{LC} \right)^{1/2} \text{ radians/sec}$$

and

$$f_{0i} \cong \frac{1}{2\pi} \left(\frac{r_i}{LC} \right)^{1/2} \text{ hertz.} \quad (29)$$

* Provided the loss factors R, G are frequency independent.

We choose the product, $LC = 6.44 \times 10^{-9}$ to yield

$$\begin{aligned}\beta_{01} &= 5,912 \text{ sec}^{-1}; & f_{01} &\cong 887 \text{ Hz} \\ \beta_{02} &= 15,708 \text{ sec}^{-1}; & f_{02} &\cong 2,487 \text{ Hz} \\ \beta_{03} &= 22,481 \text{ sec}^{-1}; & f_{03} &\cong 3,578 \text{ Hz},\end{aligned}\quad (30)$$

and a damping corresponding to

$$\alpha \cong 2330 \text{ sec}^{-1}.* \quad (31)$$

Recall that the quality factor Q for a simple resonance is $Q = (\beta/2\alpha) = f/\Delta f_{-3dB}$. The choices therefore correspond to Q 's of

$$\begin{aligned}Q_1 &\cong 1.3 \\ Q_2 &\cong 3.4 \\ Q_3 &\cong 4.8.\end{aligned}\quad (32)$$

These values are chosen to produce a filter which, when used in combination with a T1 carbon button or a WE EL-2 electret, will approximate the D-channel bank band limits.

4.1.2 Acoustic filter design—T1 uniform ladder

The next matter is how to convert the choice of α and β_{0i} 's into a physical acoustic structure. We are interested in the T1-transmitter size and the EL-2 size as existing telephone transducers. Let us consider the T1 size first. We will make this design for an experimental electret microphone having the same size as the T1-transmitter but intended to be a higher-quality replacement for the carbon button.

Some constraints then are: simplicity of fabrication; the diameter of the circular mike, namely, 46 mm; a maximum length of the filter that will allow it to fit into the conventional telephone handset; and an interest in keeping acoustic impedance levels low enough that stray losses do not dominate the intended losses. And, oh yes, watch out for shortwave effects.

A straightforward design that meets these constraints is shown in Fig. 5. The values are arrived at through the following sequence. We have already selected the product $LC = 6.44 \times 10^{-9}$ to set favorable pole positions. Now, as a convenient value, choose

$$C = 4.0 \times 10^{-6} \text{ acoustic farads,}$$

which implies

$$L = 1.61 \times 10^{-3} \text{ acoustic henries.}$$

* These choices are the results of several trial calculations for the characteristics desired for the prescribed transducers.

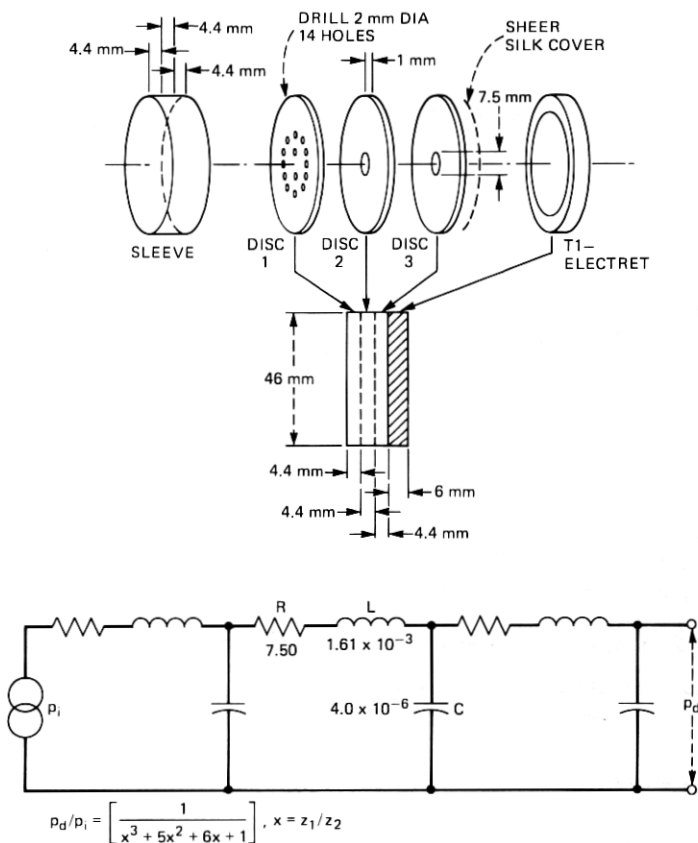


Fig. 5—Physical design of a uniform ladder acoustic filter for a T1-size electret microphone.

The choice $\alpha = 2330$, together with the intent that most loss will be supplied by R leads to

$$R = 7.5 \text{ acoustic ohms.}$$

From the lumped compliance relations (16), and the diameter of the transducer, we calculate the length of each cavity to be

$$C = \frac{\pi(4.6)^2}{4} l / \rho c^2 = 4.0 \times 10^{-6}$$

or

$$l = 0.34 \text{ cm.}$$

Similarly, from the lumped inertance relation (14), we calculate the diameter of the thin aperture to be

$$d = \rho / L = \frac{1.21 \times 10^{-3}}{1.61 \times 10^{-3}} = 0.75 \text{ cm.}$$

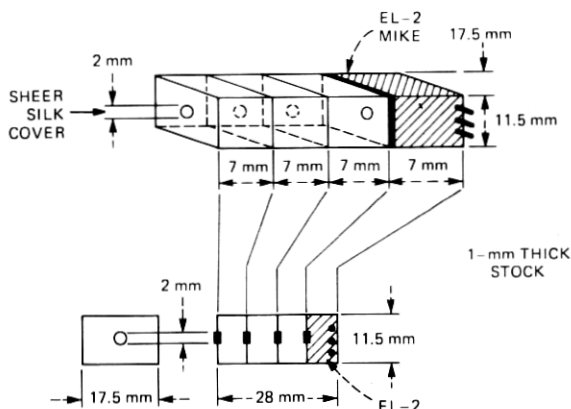


Fig. 6—Physical design of a uniform ladder acoustic filter for a WE model EL-2 electret microphone.

This aperture has an area of 0.44 cm^2 . To diminish symmetry and combat distributed effects, and to pick up additional damping, we have in this instance chosen to implement the cover-plate inertance as a group of 14 parallel holes having an open area equivalent to the single perforation.* The damping of the perforations is much less than is needed, so sheer silk cloth (128 \times 124 fibers/inch) was used to implement lumped R 's. This screen is estimated to give about 3–5 cgs ohms for 1 cm^2 area.

Also, right off, we are on guard about the large diameter of this structure—which we chose to be the easiest fit to the T1 microphone size.

Using the same fundamental design, we have two other interests. One is in placing the singularities of the filter transfer function a bit higher, so as to make the filter a bit more appropriate for a flat response transducer (rather than for the slightly rising characteristics shown in Fig. 1). Another is to apply the design to the smaller EL-2 electret, and to other microphones as well.

4.1.3 T1-9mm bore

To examine the first interest, we increased the pole frequencies by reducing the inertance values. (Note that the mechanical precision for establishing d is the same as for establishing the value of L .) We scaled the pole values up by approximately 10 percent by reducing the L

* This choice is consistent with approximating the lumped inertance as $\rho l/A$, but is not consistent with ρ/d . Several factors enter the consideration. The effective length of the aperture is more nearly $l_e = (l + 1.7a)$, and for the small holes l and a are comparable in size. Additionally, viscous effects increase the apparent inertance, as does the mutual reactance among an array of ports.

values by about 17 percent, by enlarging the openings between cavities to a 0.9-cm diameter. The damping values were maintained the same.

4.1.4 EL-2 uniform ladder

A filter design suitable for use with the EL-2 electret was also made from the uniform ladder analysis. This is easily done by noting the EL-2 dimensions, and scaling the acoustic impedance levels accordingly. Our choice for this is shown in Fig. 6, where the values represent an impedance level scaling of $\times 4$ upwards, namely,

$$L = 6.44 \times 10^{-3}$$

$$C = 1.0 \times 10^{-6}$$

$$R = 30.$$

In this case, the 2-mm aperture is used for each inertance.

4.1.5 Primo uniform ladder

The same type of impedance scaling (upward $\times 8$) leads to a similar design for the round (1-cm diameter) Primo electret microphone, as shown in Fig. 7.

4.2 Tapered ladder designs

Another approach which allows much greater flexibility in design, but which is more complicated to fabricate, is a tapered ladder design. In this case, the acoustic impedance of the filter network can be elevated in going from input to transducer diaphragm, allowing a wide range of choices for element sizes. In particular, increasing the impedance level permits smaller dimensions of the filter elements, and hence a greater freedom from cross modes and short wavelength effects. Further, if the impedance taper is substantial, each ladder section is not greatly loaded by the following one, and the singularities of the transfer function can be identified with each section of the ladder making for very simple calculation of the response. The poles can, of

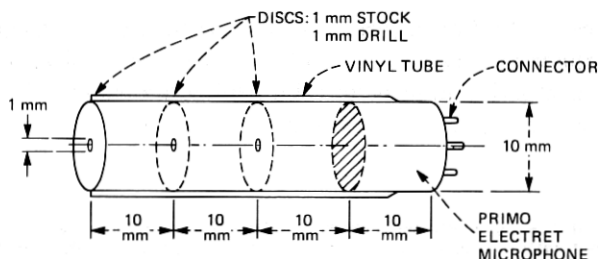


Fig. 7—Physical design of a uniform ladder acoustic filter for a Primo (Japanese manufacture) electret microphone.

course, be distributed to best advantage for a given application—which, in some instances, might be a tight cluster of poles near the band edge.*

4.3 Tapered ladder with side branch

The tapered design and the relative impedance isolation of the ladder sections permit an easy introduction of side-branch resonators. The side branch can be used to "plant" a zero of transmission in the transfer function in an advantageous way. Typically, this might be used to steepen the rate of cut-off at the band edge. This feature, of course, is obtained at the expense of the asymptotic rate of cut-off and out-of-band rejection (because the net order of the filter is effectively reduced).

A tapered design for the T1 telephone transmitter with a side branch designed to approach the D-channel bank limits is shown in Fig. 8. In this instance, the impedance level of the prototype ladder filter ascends by about a factor of 2 with each section, and the poles have all been pushed toward the 2- to 4-kHz range. The side branch modification is made to place a zero of transmission at 4 kHz, to steepen the rate of cut of the filter as 4 kHz is approached. The damping is chosen to provide pole Q 's of approximately 1.5 to 2.0 and a Q for the zero (anti-resonance) of about 10.0.

V. COMPUTED RESPONSES FOR THE ACOUSTIC FILTER DESIGNS

To explore the expected behavior of these filter designs, we wrote Fortran programs to calculate and plot the frequency-vs-amplitude and frequency-vs-phase responses. The programs also provided comparisons between the responses using a lumped-constant formulation and one using the distributed one-dimensional parameters of (16). In the latter, the cavities were represented by T-sections of trigonometric elements. Lumped inertances were retained for the apertures.†

5.1 Computed responses—uniform ladder

The log-amplitude, phase, and linear-amplitude responses vs frequency for the T1-uniform ladder network of Fig. 5 are shown in Figs. 9a to 9c. These responses are calculated for distributed one-dimensional parameters. As previously mentioned, the choice of net-

* Note, too, that other possibilities exist for implementing more complex filters. For example, the low-pass structure can be converted into a bandpass structure by introducing an aperture, or communicating air path, between the inside volume of the large cavities and the outside air. In effect, this places an inertance in parallel with each shunt compliance of the ladder network.

† The radiation impedance is taken (for computational tractability) as that for a circular piston in an infinite baffle. When the radiation impedance is overtly represented, the value of the aperture inertance at the filter face is reduced by one-half.

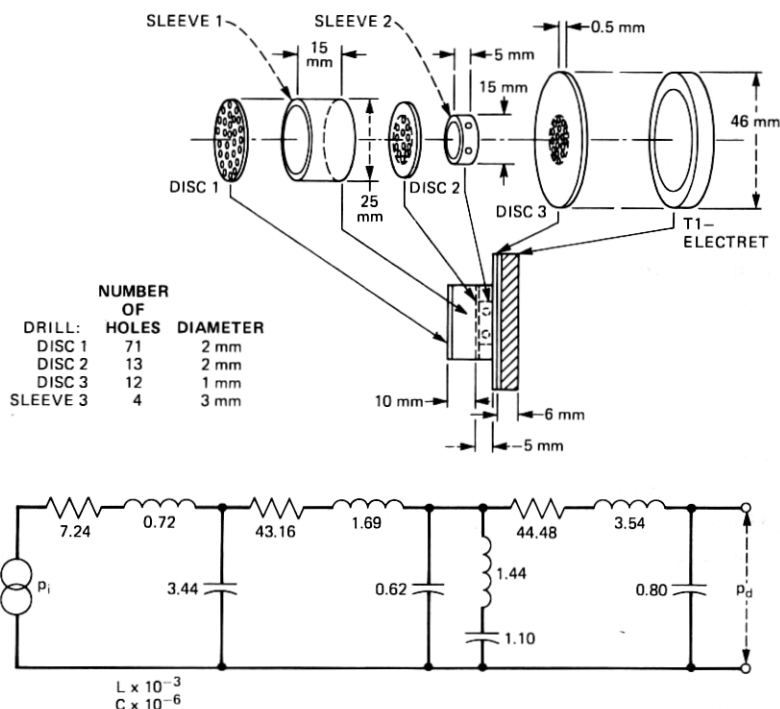


Fig. 8—Physical design of a tapered-ladder acoustic filter for a T1-size electret microphone.

work values anticipates the combined response of the filter applied to a microphone with enhanced high-frequency response.

Computation of the response using lumped and one-dimensional distributed formulations showed relatively small differences, suggesting that the arguments made about lumped approximations (for the dimensions of interest) were reasonable. The amplitude response calculated from lumped elements is shown dashed in Fig. 9c. This difference was the greatest encountered, because the T1 microphone was the largest-size transducer considered.

Note that none of the programmed (one-dimensional) wave calculations account for short wavelength cross-mode effects, which we would expect to see at frequencies around 10 kHz.

The calculated lumped-constant response of the uniform ladder design for the EL-2 electret is sensibly the same as for the T1 microphone. The designs differ only by an impedance scaling of 4. The one-dimensional distributed behaviors differ only in small detail (and only at the higher frequencies) in that, because of its smaller dimensions, the EL-2 uniform ladder is better represented by the lumped elements used for the design (i.e., distributed parameter effects are not as great in the smaller EL-2).

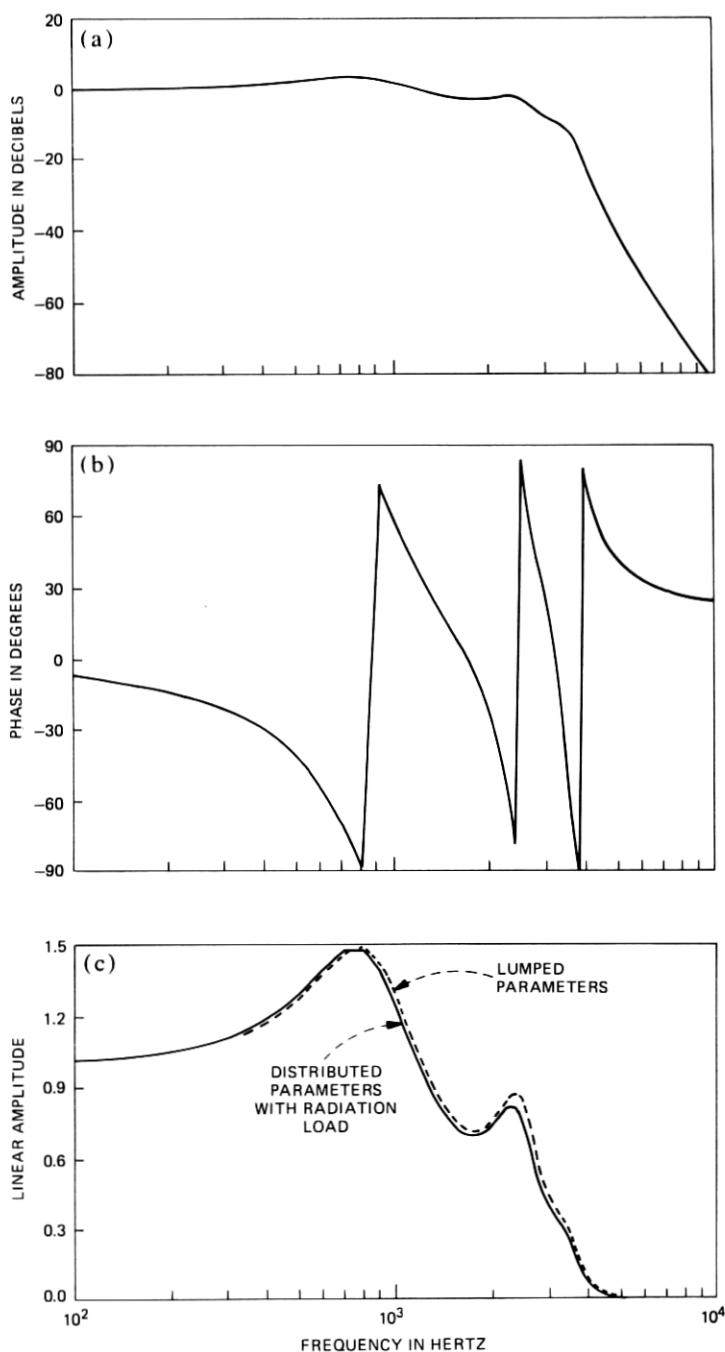


Fig. 9—Computed responses for uniform-ladder acoustic filter of Fig. 5. (a) Log amplitude response. (b) Phase response. (c) Linear amplitude response.

A calculation of the uniform ladder response with lumped parameters and small damping, specifically R 's = 0.1 cgs ohms, places the poles of the transfer function in clear evidence, as shown in Fig. 10a. The same computation with distributed parameters, radiation impedance, and small damping gives nearly the same result, shown in Fig. 10b.

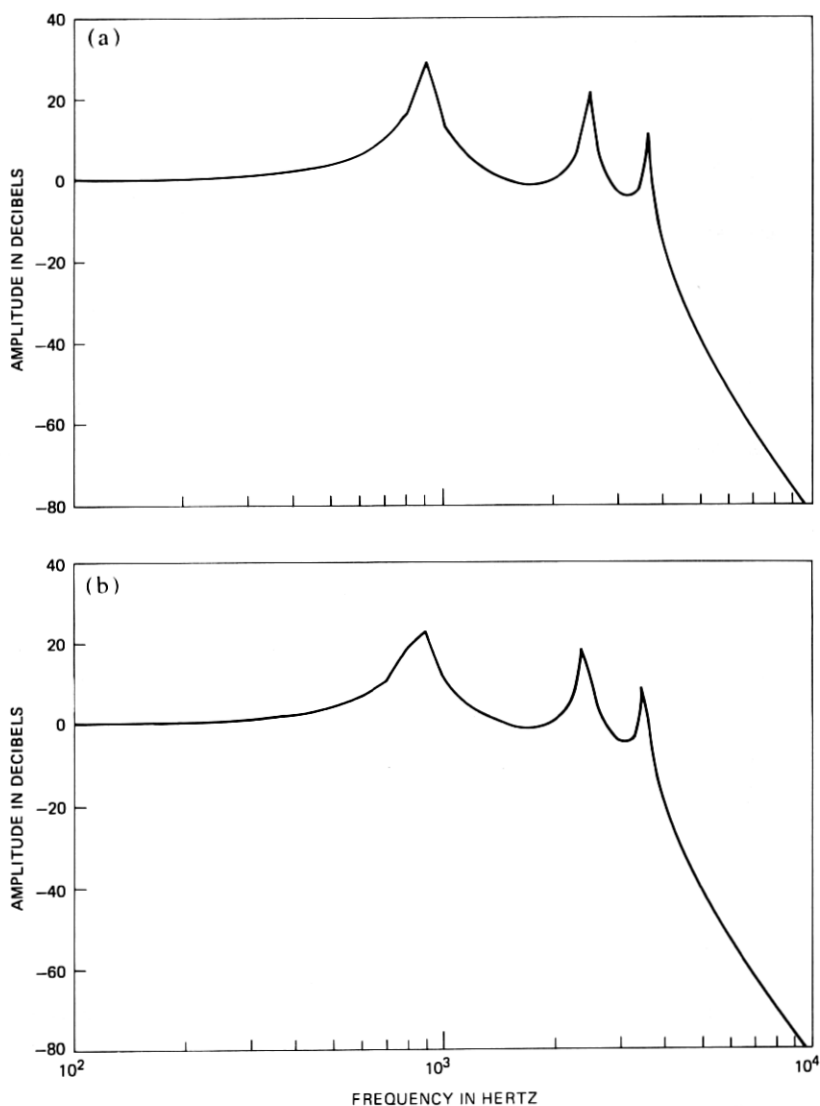


Fig. 10—Computed amplitude-frequency response for filter of Fig. 5 with low damping (R 's = 0.1 ohm). (a) Lumped parameters. (b) Distributed parameters.

In general, the poles fall approximately as designed.

A side interest in fabrication is the effect of distribution of damping in the filter. A calculation for $R_1 = 7.5$ cgs ohms and $R_2 = R_3 = 0$ is shown in Fig. 11a. The effect is to reduce the damping of all modes. The response of Figure 11c is obtained if R_1 and R_3 are interchanged, i.e., for $R_1 = R_2 = 0$, and $R_3 = 7.5$ ohms. If the damping is placed only in the center rung of the ladder ($R_1 = R_3 = 0$, $R_2 = 7.5$ ohms), the result is the response of Fig. 11b, where the second mode appears relatively underdamped

5.2 Computed responses—tapered ladder with side branch

The calculated amplitude and phase responses for the tapered ladder filter shown in Fig. 8 are given in Figs. 12a and 12b.* The effect of the side-branch zero placed at 4 kHz is readily apparent.

As an ancillary point, in hindsight, this design can be improved somewhat by reducing the size of the second rung shunt compliance (C_{2P}) in the network from its original value of 0.62×10^{-6} . This can be done by a smaller inner sleeve in the filter. A reduction to the value $C_{2P} = 0.05 \times 10^{-6}$ acoustic farads gives the improved response of Figs. 13a and 13b.

As another side point, the tapered ladder without the transmission zero also yields an effective all-pole filter. The response of the filter of Fig. 8 with the shunt resistance and inductance set to zero (i.e., $R_{2P} = XL_{2P} = 0$) gives the response of Figs. 14a and 14b.

A calculation of this response with lumped constants and low damping (R 's = 0.5) shows that the transmission poles have been pushed somewhat higher in frequency than for the uniform ladder (Fig. 15).

VI. FABRICATION OF PROTOTYPE MODELS

The model-shop machinist constructed physical filters from the drawings of Figs. 5 through 8. The models were made from brass because of the ease in machining, but, in practical application, the filters would be molded in plastic or stamped from sheet metal as part of the telephone set fabrication.

Also, for ease in making modifications for measurement, the housings of these first models were made so that assembly and disassembly could be rapidly done. This poses some dangers in that the fittings must be airtight to perform properly acoustically. Considerable care is therefore required in the experimental measurements.

The filter models as produced by the machinist are shown in Fig. 16.

* Calculated from lumped parameters.

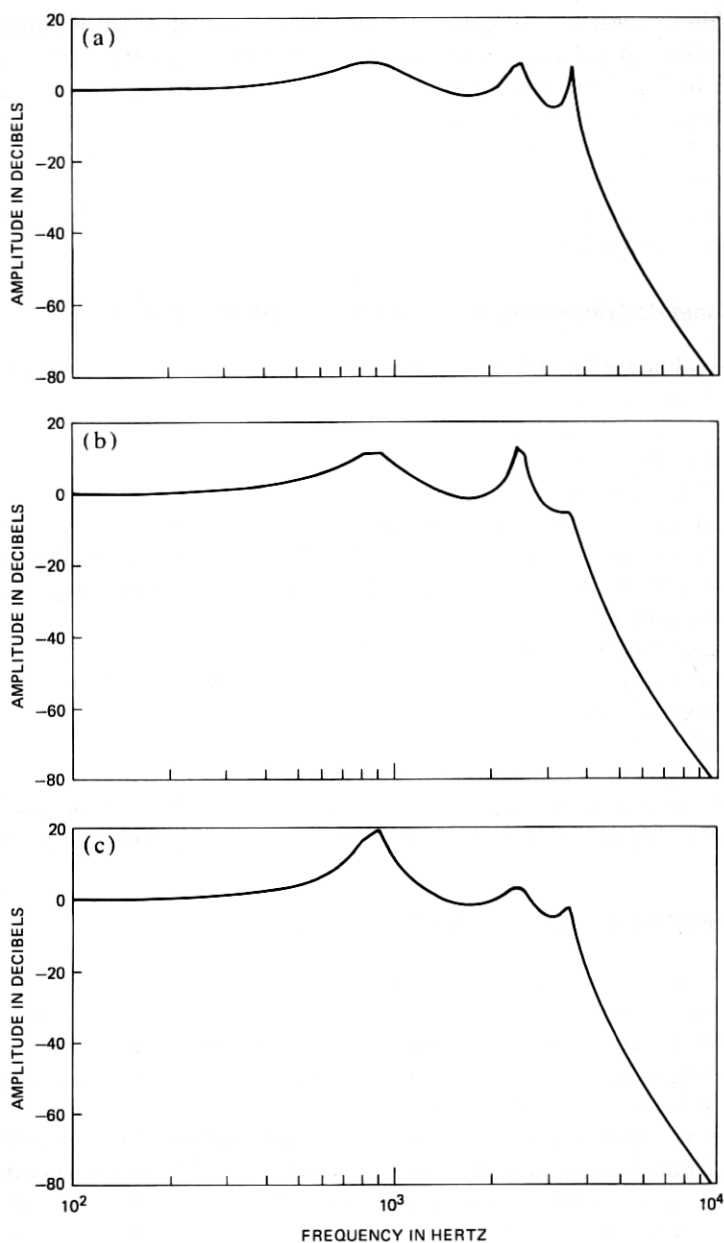


Fig. 11—Effects of location of damping (a) $R_1 = 7.5 \Omega$, $R_2 = R_3 = 0$. (b) $R_2 = 7.5 \Omega$, $R_1 = R_3 = 0$. (c) $R_1 = R_2 = 0$, $R_3 = 7.5$.

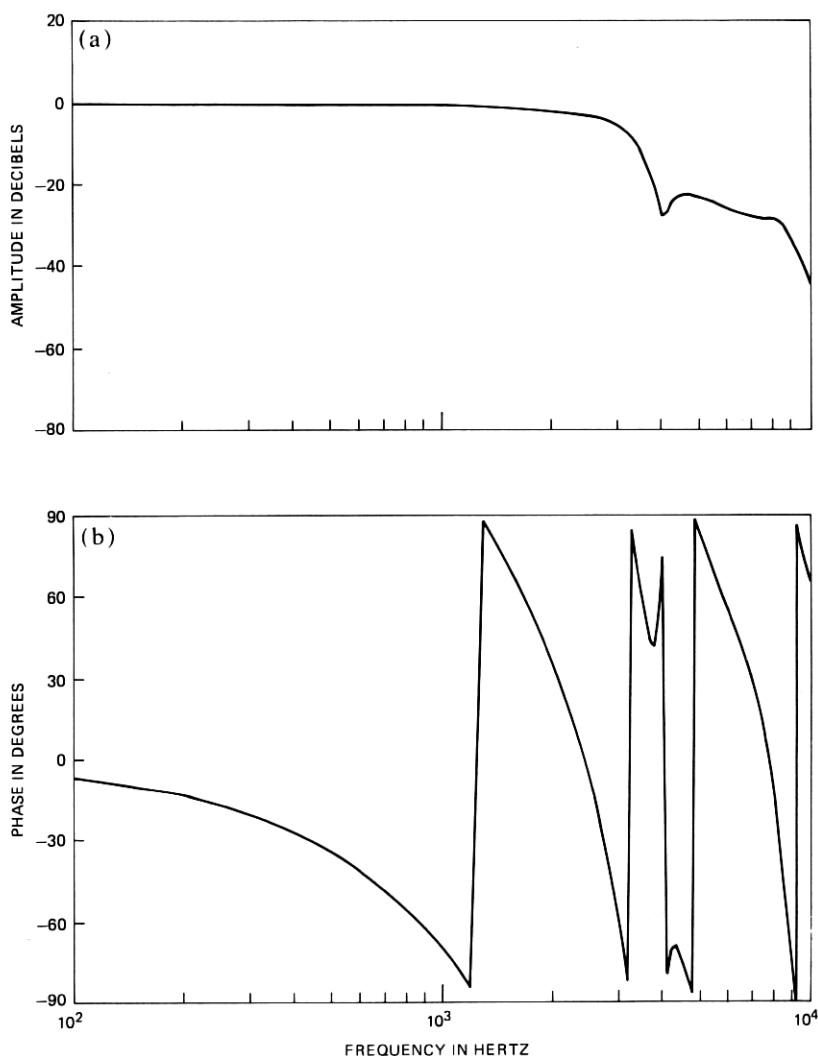


Fig. 12—Computed responses for tapered-ladder acoustic filter of Fig. 8. (a) Log amplitude response. (b) Phase response.

VII. EXPERIMENTAL MEASUREMENTS

The acoustic responses of the filter models shown in Fig. 16 were measured in the Murray Hill anechoic chamber. The experimental setup is shown in Fig. 17.

Each experimental filter and microphone was set adjacent to a calibrated condenser microphone (B&K $\frac{1}{2}$ inch). Both microphones received sound at normal incidence from an 8-inch loudspeaker source

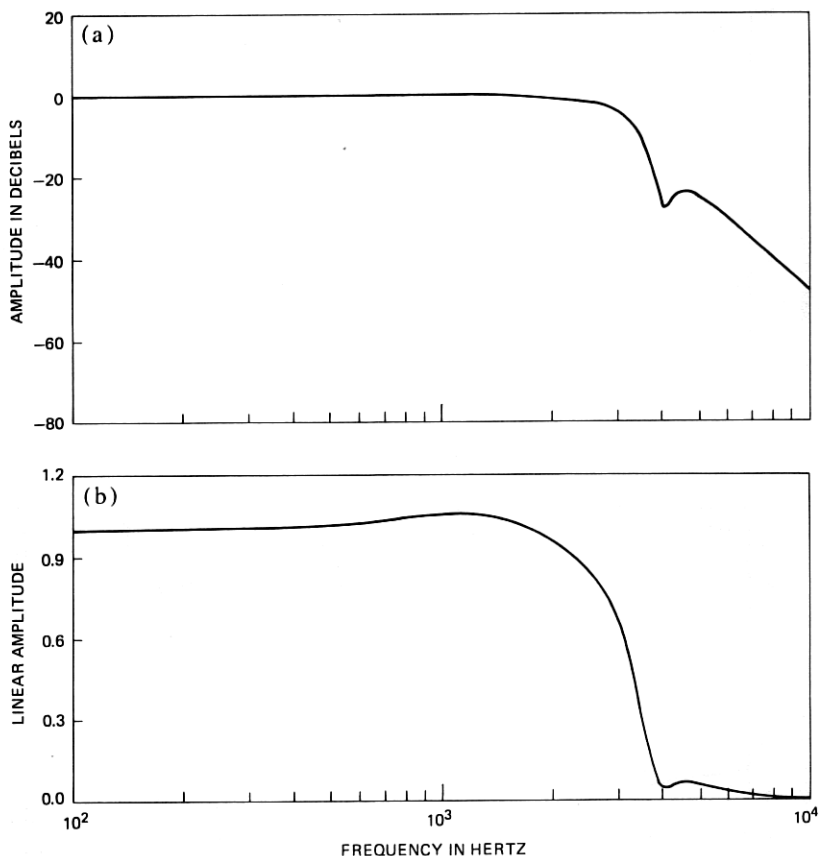


Fig. 13—Response of Fig. 12 modified by reduction in second cavity size ($C2P = 0.05 \times 10^{-6}$). (a) Log amplitude response. (b) Linear amplitude response.

2 meters away. The loudspeaker received sine-wave signals of variable frequency from a precision oscillator. Most responses were measured by maintaining a fixed sound pressure of 1 microbar at the experimental microphone. This provided a signal-to-background-noise ratio usually greater than 40 dB. In several instances, high-pass electrical filtering was used on the microphone output to eliminate ventilation noise and 60-cycle pick-up and to increase the signal-to-noise ratio to greater than 50 dB. Normally, this filtering was not used, so as not to add the electrical filter response to the microphone and acoustic filter.

7.1 Measured responses—T1 uniform ladder

The uniform ladder filter for the T1 telephone transmitter shown in Fig. 5 was fitted to an experimental electret microphone, and its response was measured with no acoustic resistances in place. This

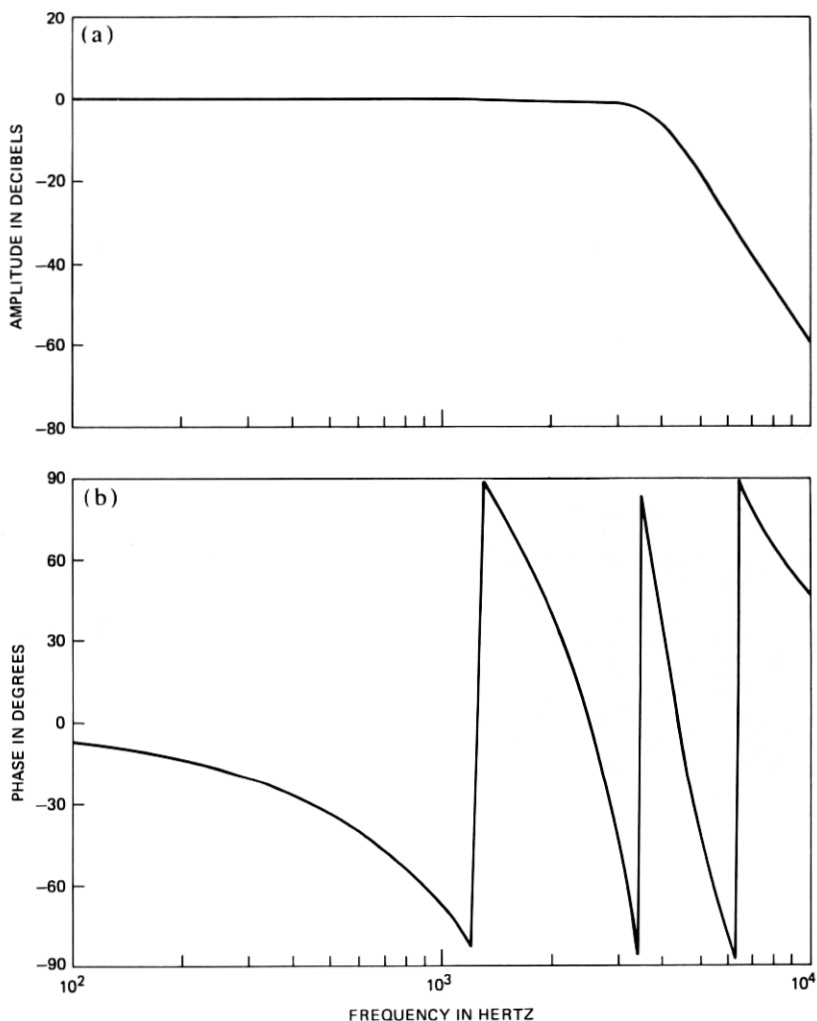


Fig. 14—Response of Fig. 12 modified by elimination of the side branch. (a) Log amplitude response. (b) Phase response.

measurement is shown in Fig. 18. The response of the microphone alone was also measured, and the difference between these curves gives the response of the acoustic filter, as shown in Fig. 19. The three mode frequencies predicted by the lumped constant design are prominent in the response.* They appear nearly where expected, but the higher two resonances are measured about 10 percent lower than where expected from lumped-constant arguments. One possible reason

* Along with a very large cross-mode response at about 10,000 Hz, to be addressed directly.

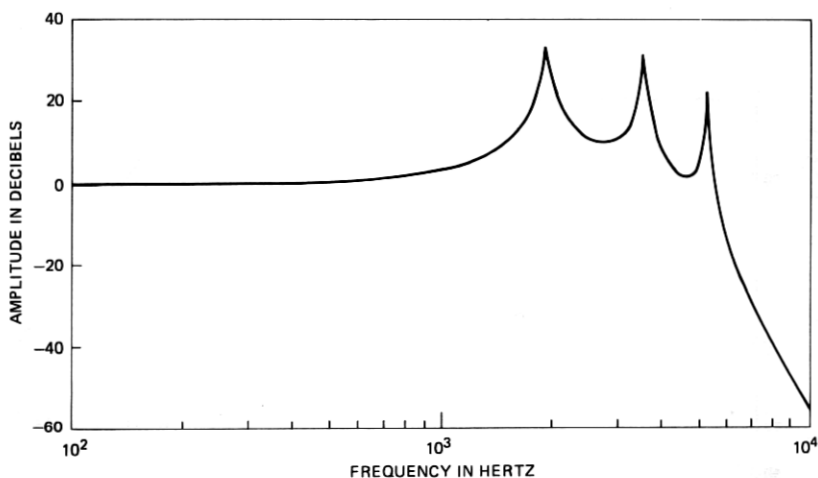


Fig. 15—Response of Fig. 14 with low damping (R 's = 0.5Ω).

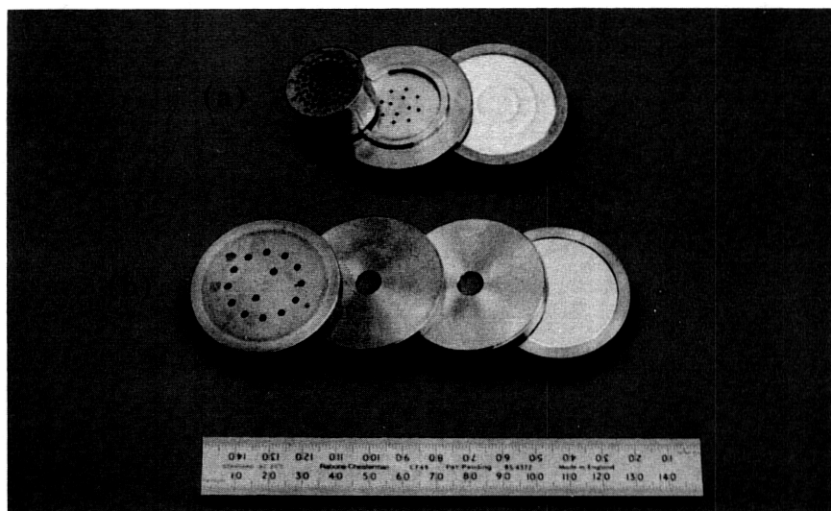


Fig. 16—Prototype acoustic filters machined in the model shop. (a) T1 tapered ladder. (b) T1 uniform ladder. (*continued on page 929*)

is that the simple relation $L_a = \rho/2a$ yields a larger value than desired. (This is supported by the “end effect” radiation reactance point of view that leads to $L_a = 0.54 \rho/a$, which says that an aperture of radius a gives an inductance 8 percent greater than the traditional $\rho/2a$ value*).

Note also, in the response without damping, the tremendous high-

* Viscous behavior in the apertures also contributes to the apparent inductance.

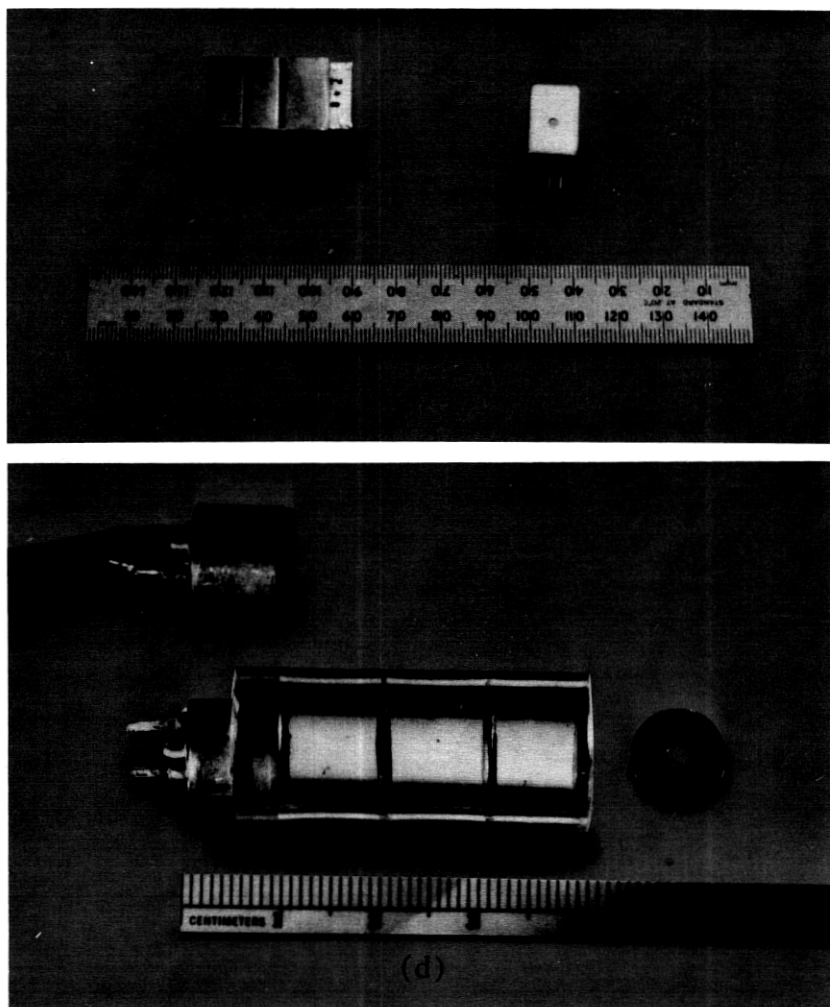


Fig. 16 (continued)—(c) EL-2 uniform ladder. (d) Primo uniform ladder.

frequency peak at about 10 kHz. Recall from Fig. 5 that the diameter of the circular microphone and acoustic filter is 46 mm. (In the inner chamber, this is reduced by the thickness of the walls to approximately 44 mm.) The overall length of the communicating chambers of the acoustic filter is $[(3.4 \text{ mm} \times 3) + 2 \text{ mm}] = 12.2 \text{ mm}$. Considering the whole structure as a cylindrical enclosure, we can use eq. (23) to calculate the expected normal modes. We need additionally only the roots of

$$\frac{d}{d\alpha} J_m(\pi\alpha) = 0.$$

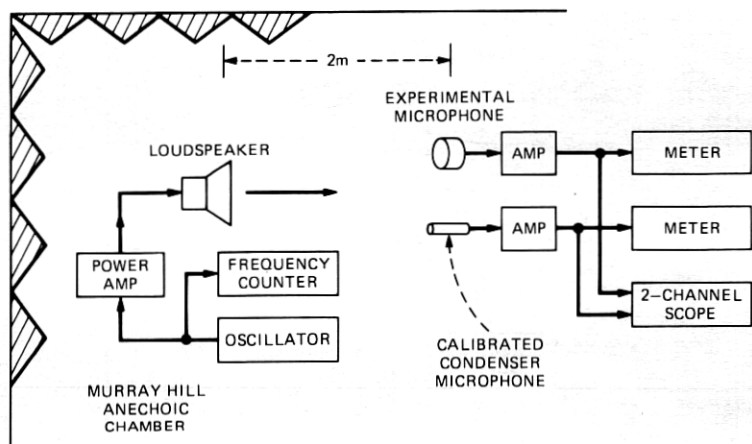


Fig. 17—Arrangement of laboratory equipment for experimental measurements in the anechoic chamber.

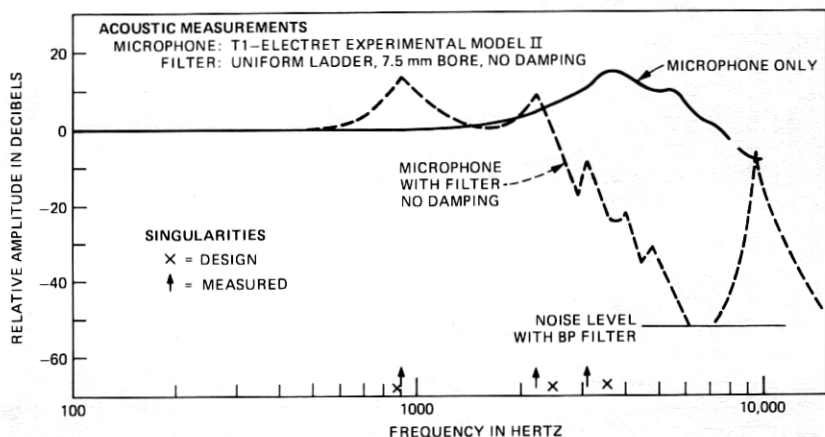


Fig. 18—Measured response of the T1-uniform ladder filter with no damping and its electret microphone.

The first few values of α_{mn} are shown in Table I. Equation (23) therefore gives the eigenfrequencies in Table II. Because the cavities really communicate only through the apertures, the length dimension mode for $l = 12.2$ mm is not readily excited. Even if it were, it is relatively high in frequency—largely well out of the speech frequency range.* If the effective length dimension is taken perhaps more realistically as equal to a single cavity thickness, then the first z -direction mode is put at 50 kHz.

* The nature of the speech signal spectrum, which typically diminishes at -6 to -12 dB per octave at high frequencies, also helps to de-emphasize the effects of high frequency modes.

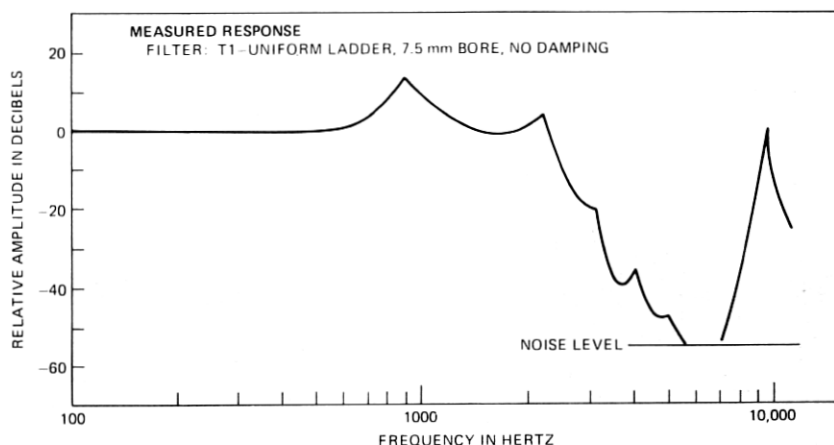


Fig. 19—Measured response of the T1-uniform ladder filter, 7.5-mm bore, no damping.

Table I

m/n	0	1	2
0	0	1.22	2.33
1	0.59	1.70	2.71
2	0.97	2.13	3.17

Table II

Mode number			Frequency (hertz)*
n_z	m	n	$f = (f_z^2 + f_r^2)^{1/2}$
0	0	0	0
1	0	0	13,934
0	1	0	4,361
0	0	1	9,017
1	1	0	14,601
1	0	1	16,597
0	1	1	12,565
1	1	1	18,763

* For 46-mm diameter.

The lowest indicated mode is the (0, 1, 0) mode at 4331 Hz. Recall that the (n_z, m, n) convention is such that the m, n th wave has m plane nodal surfaces extending radially from the axis, and n cylindrical nodes concentric with the axis. The m -waves correspond to standing pressure waves in the ϕ -direction and the n -waves correspond to radial standing waves of pressure in the r -direction. The geometry of the filter is such that the m -waves might be expected to be difficult to excite. If the (0, 1, 0) mode is excited, it is relatively weak and possibly shows up as a slight peak in the response near 4000 Hz.† The first radial mode (0, 0, 1), however, is a different story, and the center

† A similar argument might be given for the 0, 2, 0 mode at 7,170 Hz.

aperture seems favorable for exciting this mode strongly in one or more of the cavities. This mode appears to account for the truly sizeable high frequency response between 9 and 10 kHz. In realizing a useful filter of dimensions this large, therefore, considerable attention needs to be given this mode. Other modes seem well out of the speech frequency range.

In damping this particularly undesirable $(0, 0, 1)$ mode for this filter

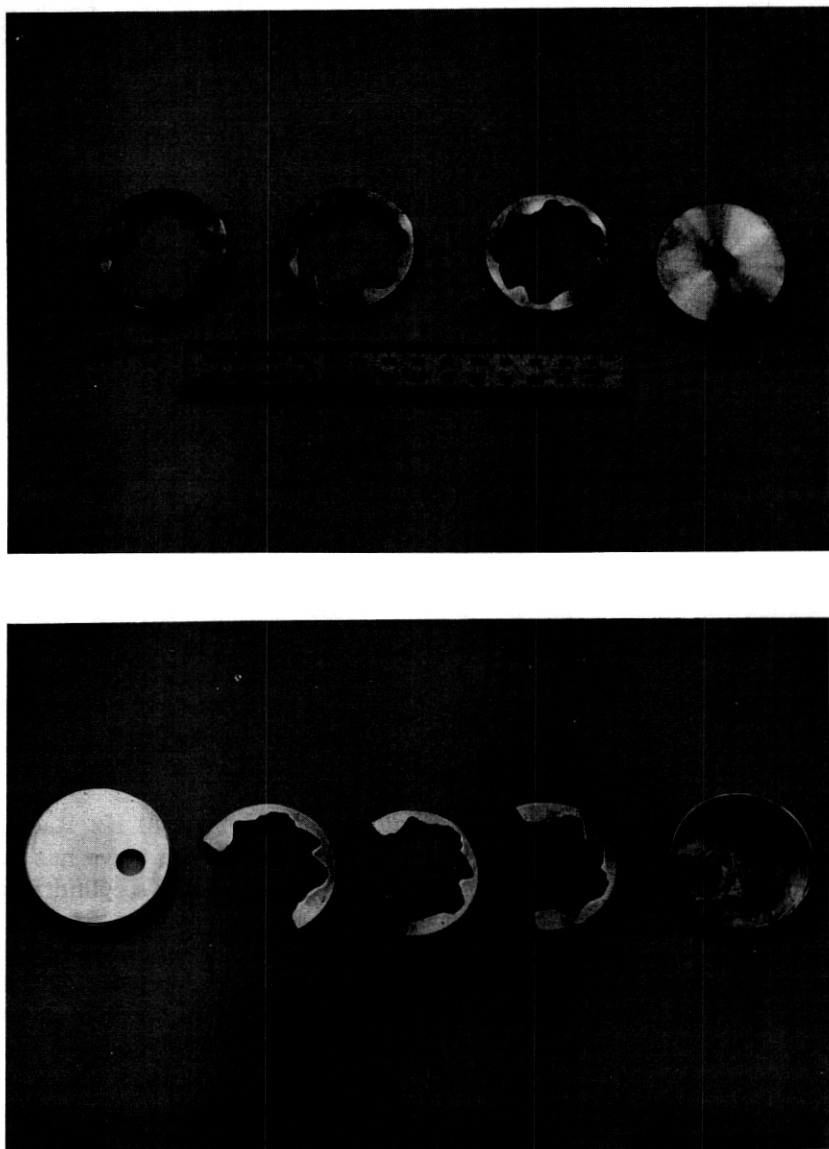


Fig. 20—Brass rings (cavity inserts) cut with irregular radii.

size, we recall the mode energy is most effectively absorbed by sound absorptive material placed near pressure maxima, and that reduction of the radial symmetry would suppress its excitation.

As a very simple expedient to reduce radial symmetry, we can introduce an irregular inner surface into the cavities by means of some brass rings cut with a random radius. A set of such rings is shown in Fig. 20a. The symmetry can be even more affected by using only the $\frac{1}{2}$ arc rings of Fig. 20b. The random radius is selected to look "rough" at wavelengths corresponding to about 10 kHz. The volume displacement of the rings is small enough that the cavity volume, and hence the acoustic capacity, is not changed much from the original design value. We can also include the prescribed silk-screen resistors in the

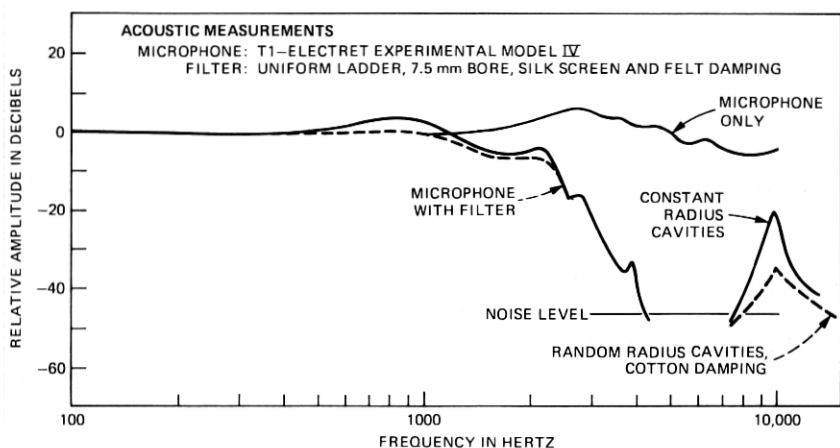


Fig. 21—Measured response of the T1-uniform ladder filter 7.5-mm bore, with damping and its electret microphone.

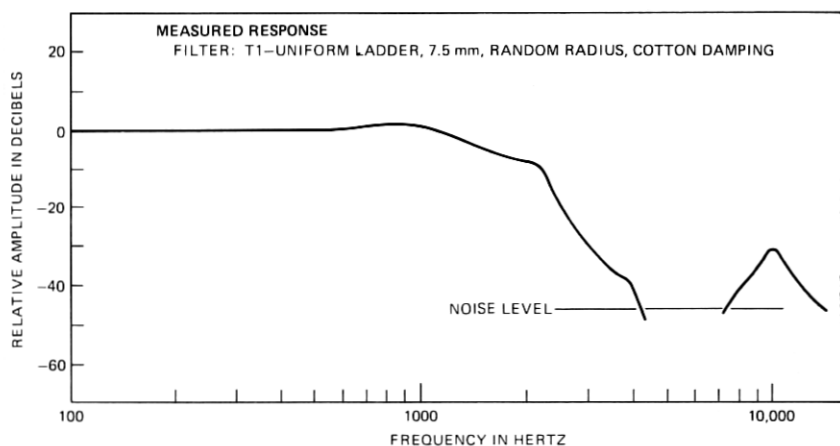


Fig. 22—Measured response of the T1-uniform filter, 7.5-mm bore, with mode suppression.

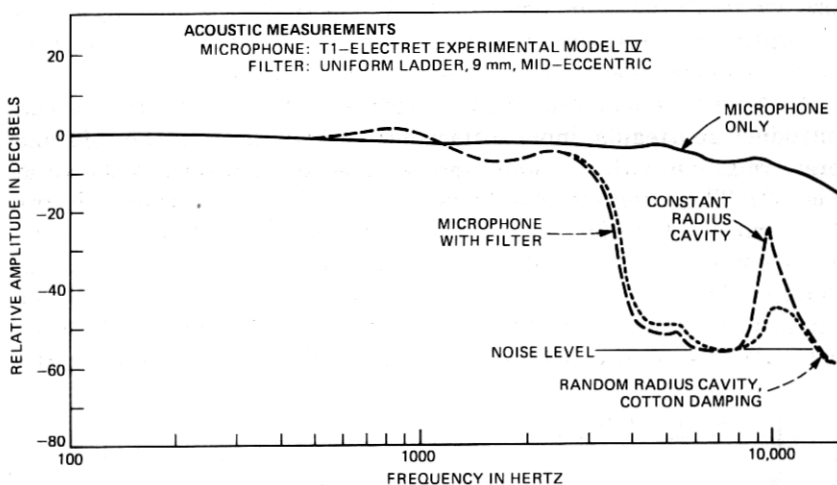


Fig. 23—Measured response of the T1-uniform ladder, 9-mm bore, and its microphone.

apertures, as well as a small amount of absorbent cotton in the cavity and cotton felt strips around the periphery. When this is done, the response of the radial mode is brought more under control, as shown by Figs. 21 and 22. This situation can be improved a bit more, even keeping the large T1 dimensions.*

The underestimate of the inertances, as discussed previously, together with the design objective that uses a microphone response rising at the high frequencies, gives us a filter that cuts off at fairly low frequencies. A 20-percent increase in the bore radius of the apertures should give an inertance reduction of 17 percent and an increase in pole frequencies of 10 percent. In addition, we can reduce the possibility for (0, 0, 1) mode excitation by placing at least one of the apertures (the center one here) off center (as shown in Fig. 20). The response of this T1-size uniform ladder is given in Figs. 23 and 24, where one sees the out-of-band rejection is successfully held at -40 dB.

7.2 Measured responses—tapered ladder with side branch

The filter design of Fig. 8 has some dimensions that are smaller (and hence less susceptible to distributed effects), but the final cavity is left with the 44-mm inner diameter.

The measured response of this filter is shown in Figs. 25 and 26.†

* A number of other possibilities exist for controlling cross-mode behavior. Their effectiveness and sophistication depend upon the willingness to complicate the physical construction of the filter. All depend upon minimizing symmetry and reducing dimensions of the acoustic elements. Straightforward approaches include enclosures having nonparallel, asymmetric, incommensurate walls, and internal partitioning to implement the overall filter as a number of smaller-sized filters in parallel. Several preliminary implementations of these notions yield significant suppression of cross modes.

† Differences among microphone-only responses are conditioned largely by differences in clamping tension for repeated installations in the experimental holder.

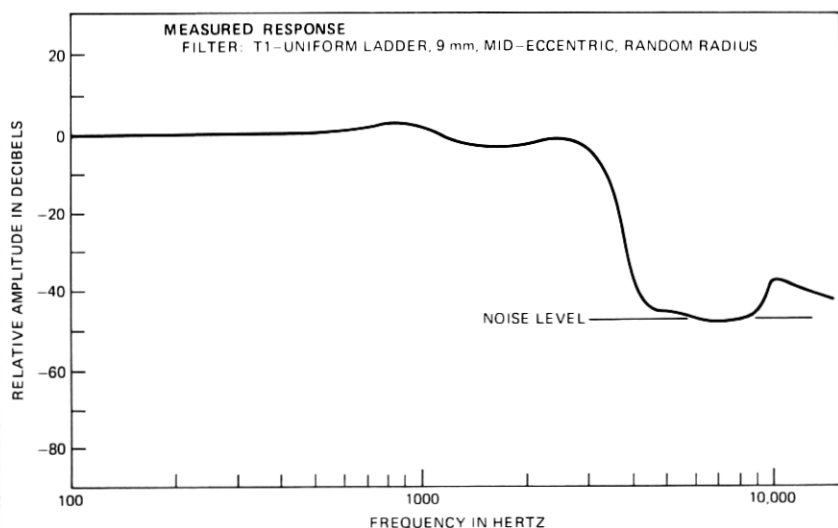


Fig. 24—Filter response only for Fig. 23.

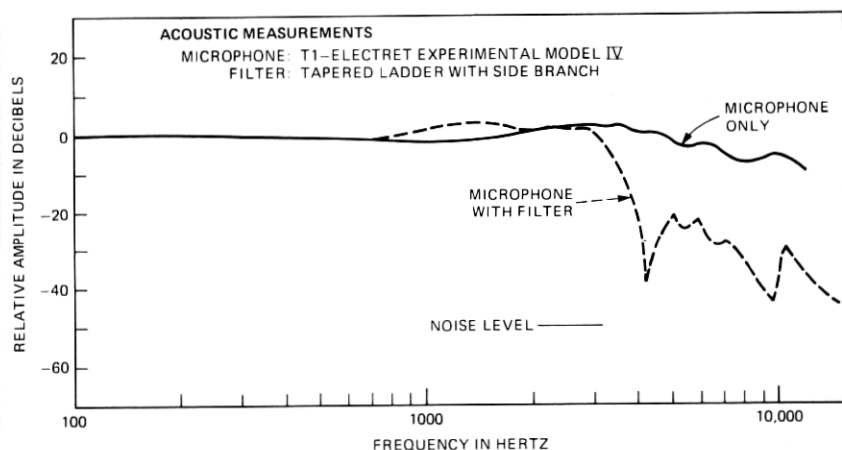


Fig. 25—Measured response of tapered ladder filter and its microphone.

The transmission zero, provided by the side branch resonator, falls approximately at the design frequency, 4000 Hz. The "recovery" in response following the zero is predicted from the lumped constant theory, but the relatively modest peak in response near 10,000 Hz is with high probability the (0, 0, 1) mode of the inner cavity.

7.3 Measured responses—EL-2 uniform ladder

Because of the smaller dimensions of the EL-2 electret microphone, short wavelength effects are substantially less bothersome, although they are not altogether absent. We implemented this filter only with the prescribed silk-screen damping in the inertive apertures. No additional cavity damping was included.

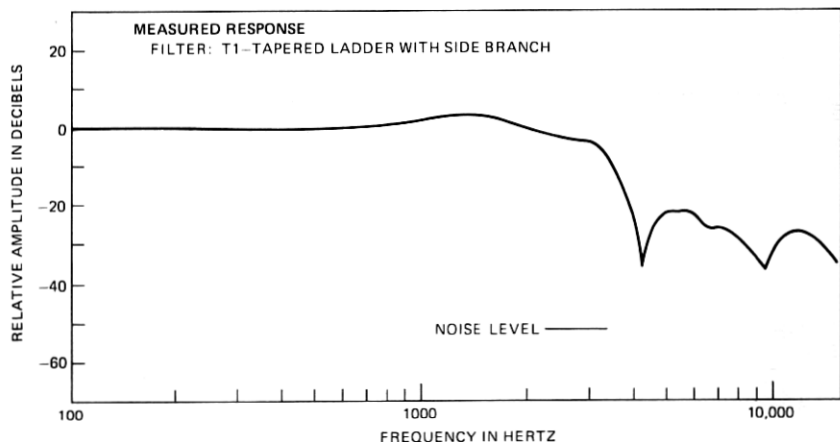


Fig. 26—Response of tapered ladder filter only.

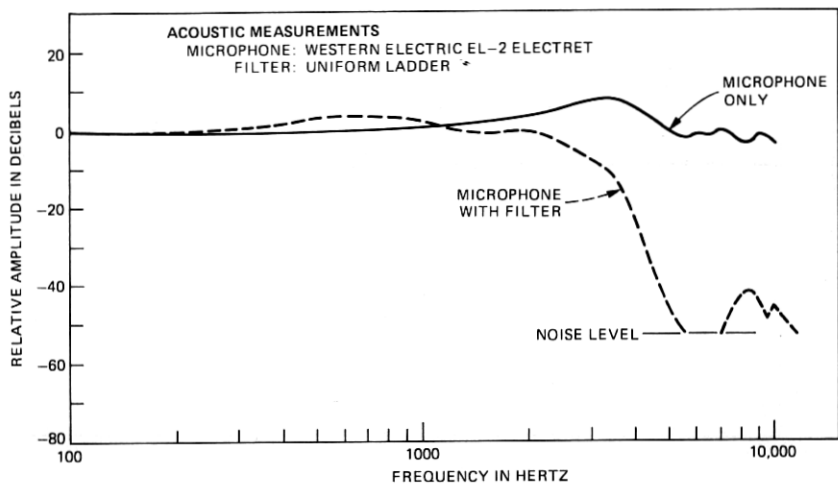


Fig. 27—Measured response of EL-2 uniform ladder and its microphone.

The EL-2 responses are shown in Figs. 27 and 28. From eq. (20), the expected mode structure can be estimated. If the length (z -dimension) of the total cavity is taken as $(3 \times 7) = 21$ mm,* together with the width and height 17.5 and 11.5 mm, respectively, the rectangular modes from eq. (20) are as shown in Table III.† The eigenfrequencies are, as previously indicated, $f = [(f_x)^2 + (f_y)^2 + (f_z)^2]^{1/2}$. The total length (z -direction) mode (0, 0, 1) and the first x -direction mode (1, 0, 0) appear to have correlates in the measured response. Even so, and

* This length is, of course, partitioned by the apertures.

† If l is taken only as the individual cavity length, the (0, 0, 1) mode is 24,286 Hz.

Table III

Mode number	Frequency (hertz)		
	f_x	f_y	f_z
0	0	0	0
1	9,714	14,783	8,095
2	19,428	29,566	48,571

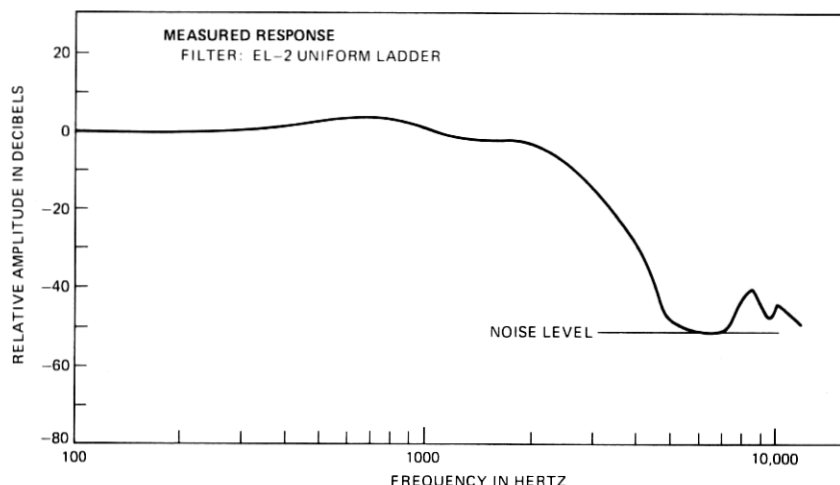


Fig. 28—Response of EL-2 uniform ladder only.

with only the serial resistor (silk-screen) damping, the out-of-band rejection is held at -40 dB.

VIII. COMPARISON OF THEORETICAL AND MEASURED RESPONSES

The measured response for the uniform ladder is best exemplified by the EL-2 and T1 designs. Measured responses compared to the computed response based only on one-dimensional sound propagation are shown in Figs. 29a and 29b.

The same comparison for the T1-size tapered ladder with side branch is shown in Fig. 30. To the extent that the one-dimensional design assumptions apply, the agreement appears satisfactory.

IX. COMPARISON OF MEASURED FILTER RESPONSES TO D-CHANNEL BANK SPECIFICATIONS

Specifications of D-channel banks band-limits for voice digitization (at least, as of October 1976)¹ are shown in Fig. 31. The tolerances are quite small—unrealistically so in terms of the variability in amplitude response of mass-produced telephone transmitters (and also in terms of the variability introduced by directional effects of the sound

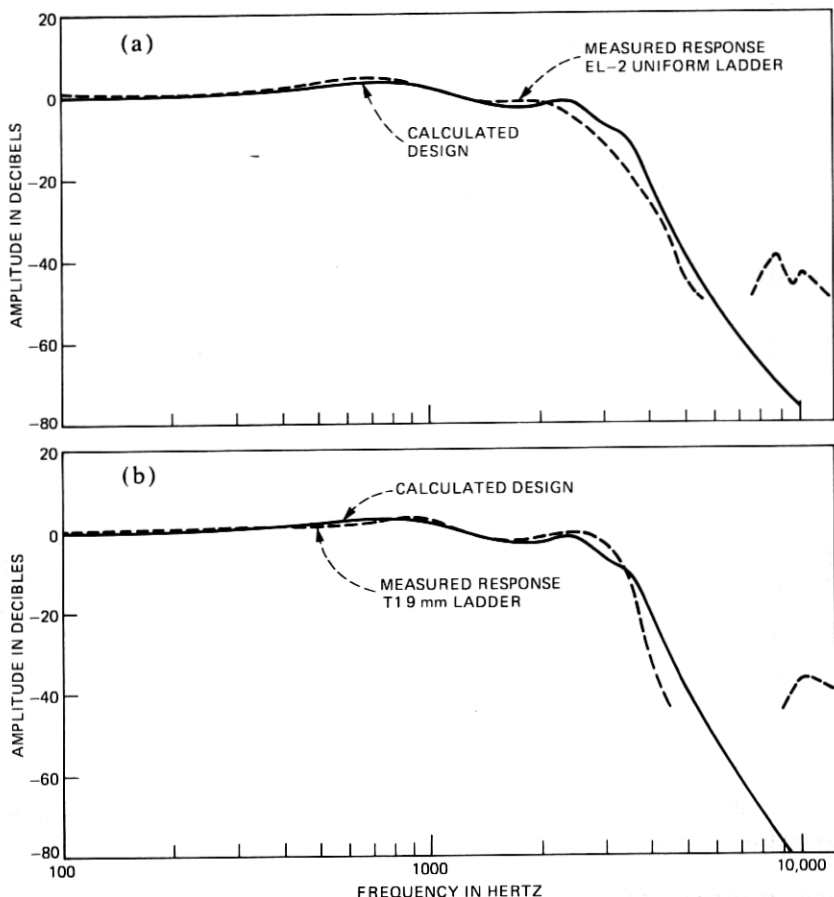


Fig. 29—Comparison between calculated design and measured response for (a) the EL-2 and (b) the T1 uniform ladder acoustic filter.

source).^{*} Nevertheless, we wish to see how closely we can approximate this characteristic with acoustic filters only.

The response of the T1-size uniform ladder with 9-mm bore is shown in Fig. 32. This comparison is for the filter response only, and assumes that it is used with a flat (uniform) response microphone.

The T1-size tapered ladder filter response is shown in Fig. 33. This response does not satisfy the D-channel bank limits, but needs some additional amount of attenuation at the higher frequencies. For example, increasing the order of the filter by two (by adding one more resonator section) would give an out-of-band rejection satisfactory to the specifications.

^{*} These tolerances are implied, at least in part, by transmission objectives for multiple tandeming of voice circuits.

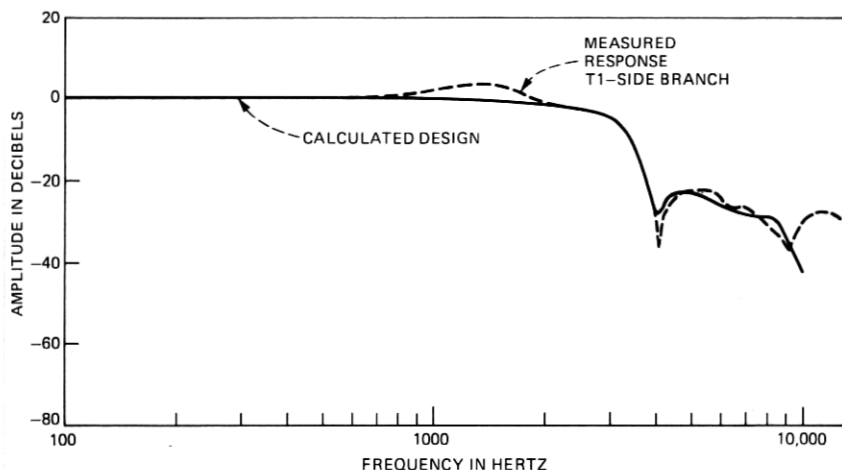


Fig. 30—Comparison between calculated design and measured response for the T1-tapered ladder filter.

The uniform ladder filter, used in combination with the Western Electric EL-2 electret microphone, does a passably good job of approximating the D-channel bank specification. This response is shown in Fig. 34. Some further adjustment of the design and of the damping might make the fit even closer.

X. CONCLUSION

This study has put forward the suggestion that a large part, or even all, of the band limitation required for digitization of acoustic signals can be accomplished by relatively simple acoustic filters. Moreover, the acoustic filters can be used as an appliqué to the signal transducer, both for transmission and reception. In a highly economical form, the filters can be implemented as part of the transducer housing—injection molded as part of the transmitter cap in a conventional telephone handset, or stamped as part of the transducer cover in other cases.

The study also establishes straightforward design theory for voice-band acoustic filters. Further, it shows how one-dimensional wave treatment and lumped characterization, if prudently applied, give computationally convenient guideposts for implementing the physical filters.

Finally, the design procedure is applied to electret microphones of the T1 size and the Western Electric model EL-2 size. The expected frequency responses of the designs are computed, and the physical filters are machined in the model shop. These prototypes are set up in the anechoic chamber, and their frequency behavior is measured. The results demonstrate that relatively simple acoustic structures can approximate the D-channel bank filter specifications for voice digiti-

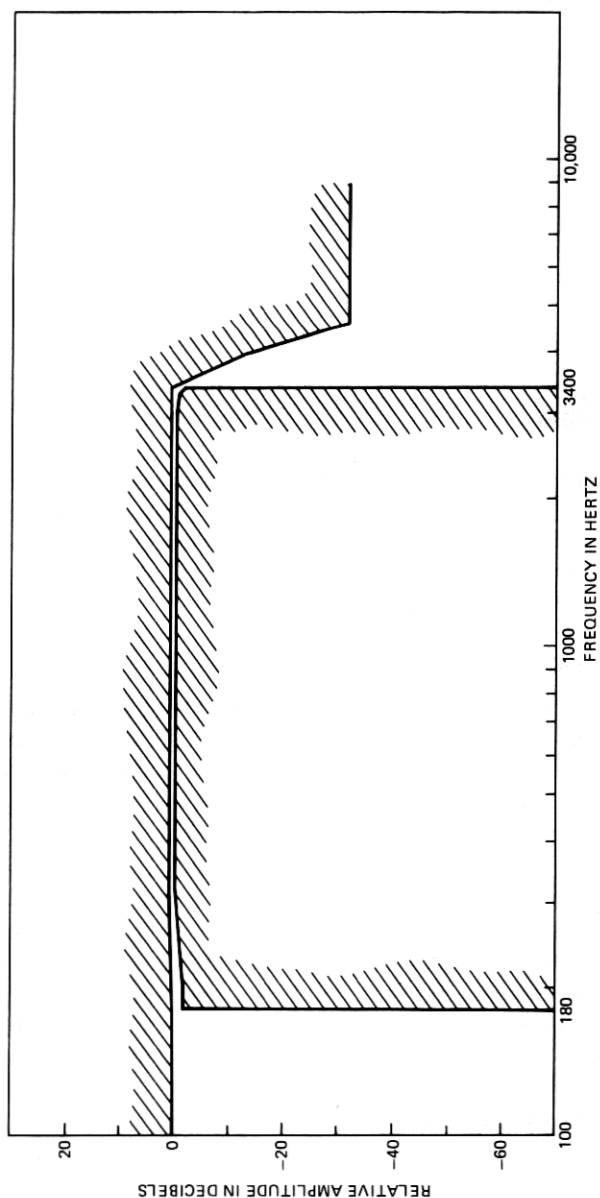


Fig. 31—Amplitude vs frequency response specification for D-channel bank band limitation [October 1976 (Ref. 1)].

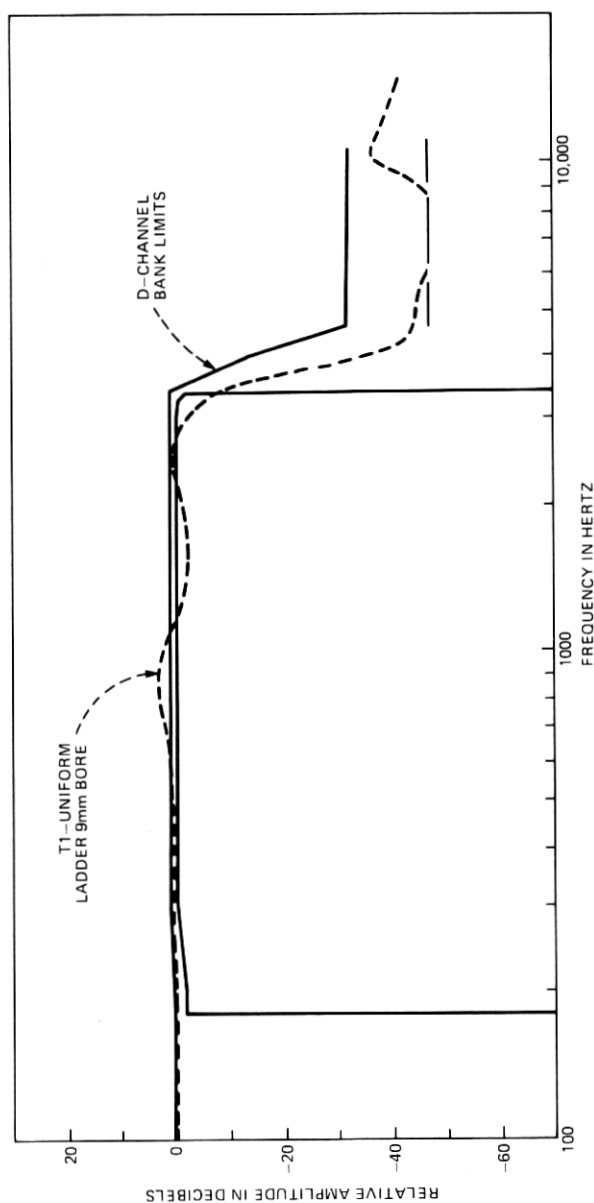


Fig. 32—Comparison of 9-mm uniform ladder response to D-bank specification.

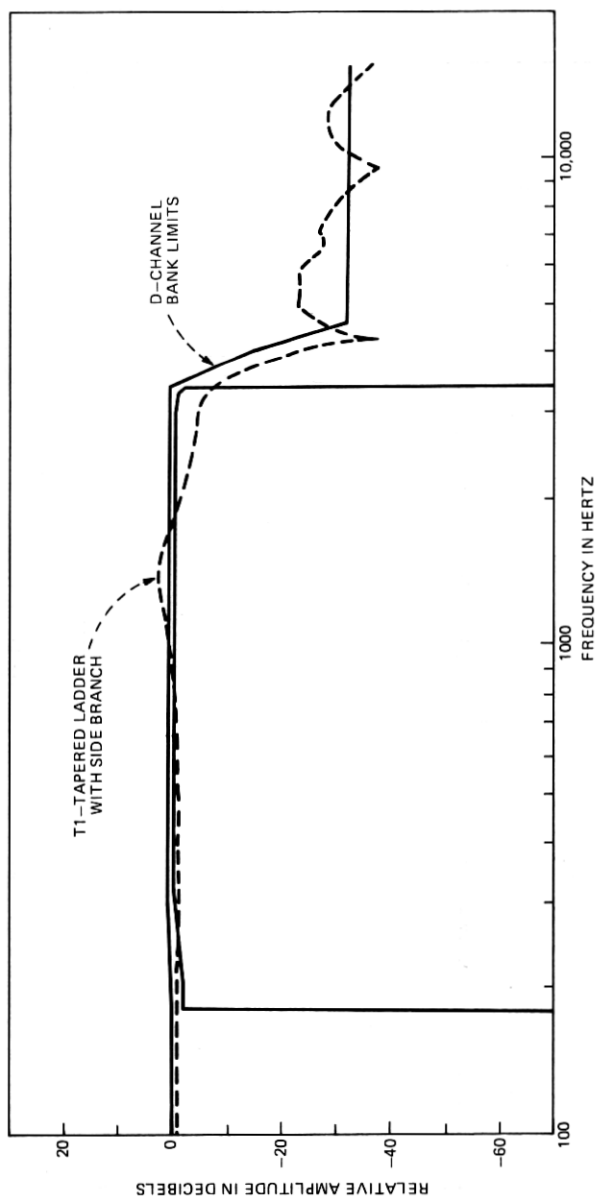


Fig. 33—Comparison of tapered ladder response to D-bank specification.

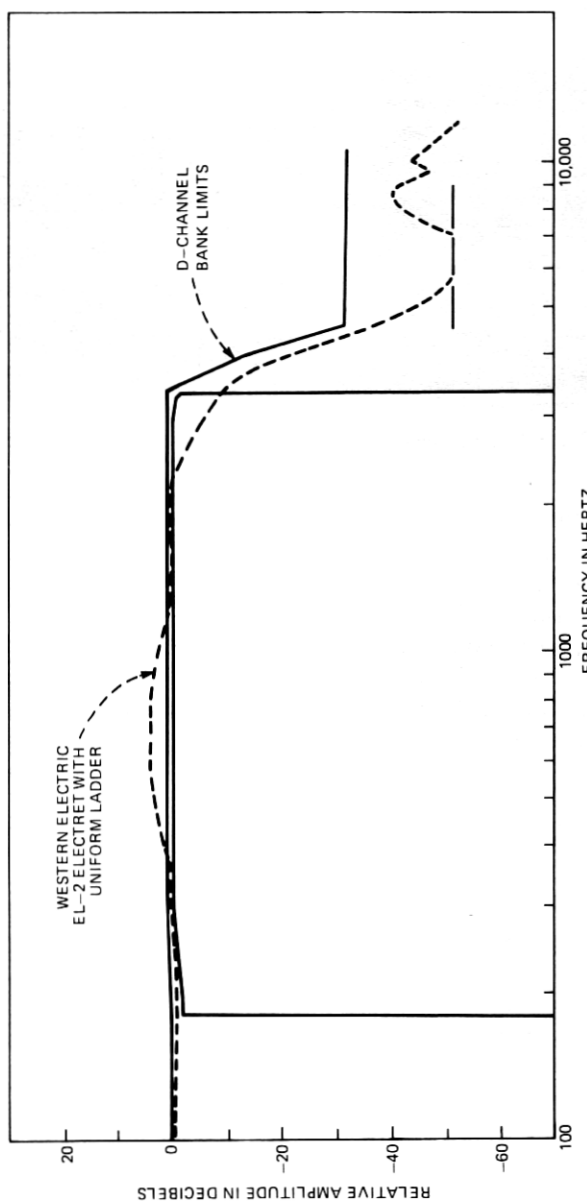


Fig. 34—Comparison of the EL-2 uniform ladder acoustic filter response to the D-channel bank filter specification.



Fig. 35—Office telephone (Mod. 2565HK) with experimental acoustic filter and electret microphone installed.

zation. Tolerances in physical dimensions are comfortable, and are virtually the same as in the elements of the electrical counterpart. Informal real-telephone testing of the prototypes lends additional confidence to the conclusions.*

Therefore, for the digitization of voice, and other acoustic signals as well, the use of band-limiting acoustic filters appears feasible and potentially attractive. The filters are simple, are highly linear, require no power, have no moving parts, and are inexpensive. They are only filled with air.

XI. ACKNOWLEDGMENTS

I thank J. West and R. Kubli of the Acoustics Research Department for giving me laboratory instruments to make the experimental measurements described in Section VII. I thank machinist Herman Stern for fabricating the several prototype filter models described in Section VI. And I thank my son James for helping me make the free-field measurements in the anechoic chamber.

REFERENCES

1. C. R. Baugh, unpublished work.
2. Unpublished experimental data, Bell Laboratories Branch Laboratory, Indianapolis.
3. P. M. Morse and U. Ingard, *Theoretical Acoustics*, New York: McGraw-Hill, 1968.
4. J. L. Flanagan, *Speech Analysis, Synthesis and Perception*, 2nd ed. New York: Springer Verlag, 1972.

* The author has used the 7.5-mm, T1-uniform filter in his office telephone for the past several months. The filter and an experimental T1-size electret transmitter are shown in Fig. 35.